Development of a dynamic model of a BWR nuclear power plant. Part II: The dynamic model

Nonbøl, Erik

Publication date:
1975

Document Version
Publisher's PDF, also known as Version of record

Risø Report No. 336

Risø Report No. 336

Danish Atomic Energy Commission

Research Establishment Risø

Development of a Dynamic Model of a BWR Nuclear Power Plant

Part II: The Dynamic Model

by Erik Nonbøl

December 1975

Sales distributors: Jul. Gjellerup, 87, Sølvgade, DK-1307 Copenhagen K, Denmark

Available on exchange from: Library, Danish Atomic Energy Commission, Risø, DK-4000 Roskilde, Denmark

INIS Descriptors

B CODES
BWR TYPE REACTORS
FEEDWATER
FEEDWATER HEATERS
HEATERS
MATHEMATICAL MODELS
NUCLEAR POWER PLANTS
ONE-DIMENSIONAL CALCULATIONS
PUMPS
REACTOR CONTROL SYSTEMS
REACTOR KINETICS EQUATIONS
REACTOR OPERATION
REACTOR SIMULATORS
STEAM CONDENSERS
STEAM TURBINES
TRANSIENTS

UDC 621.039.524-97: 621.039.51: 681.3.06

December 1975 Risø Report No. 336

Development of a Dynamic Model of a BWR Nuclear Power Plant

Part II: The Dynamic Model

by

Erik Nonbøl

Danish Atomic Energy Commission
Research Establishment Risø
Department of Reactor Technology

Abstract

A dynamic model of a nuclear power plant, including a boiling water reactor, high- and low-pressure turbines, moisture separator, reheater, condenser, feedwater heaters and feedwater pump, was developed. The model is one-dimensional except for the nuclear part of the reactor, which is based on the point kinetics equation, and the condenser model and feedwater pump model. It has been used to study different transients occurring during normal operating conditions and for evaluating the control systems of a BWR nuclear power plant. Particular emphasis was laid on the reactor pressure control system and the recirculation flow control system.

This report was written in partial fulfilment of the requirements for obtaining the lic. techn. (Ph.D.) degree.

ISBN 87-550-0405-9

CONTENTS

Page

1. INTRODUCTION

When studying different transients that may occur in a nuclear power plant, it is useful to have a mathematical model which can simulate the behaviour of the whole plant. It can be used to ensure that the plant operates, under normal conditions, within the limits set by the authorities. The control system can also be designed on the basis of such a model.

When making a model of a whole power plant it is a problem to decide how many parts of the plant it is necessary to include to get a fairly realistic model. Having decided this point, one must then decide to what extent all parts of the model must be detailed. Because of the long computing times involved when using such models, it is not always desirable to include all details.

The model available comprises a boiling-water reactor, a high-pressure turbine and a low-pressure turbine, a moisture separator and reheater, a condenser, feedwater heaters and feedwater pump. The nuclear part of the reactor model is based on the point kinetics equation, whereas the boiling part is based on one cooling channel and treated one-dimensionally. The turbine model is one-dimensional and rather detailed because of its great importance in a dynamic sense. Moisture separator, reheater and feedwater heaters are also treated one-dimensionally. Condenser and feedwater pump are point models. Different valves such as the turbine inlet regulation valve, reheater regulation valve, level regulation valves for condensate in the moisture separator, reheater and feedwater heaters, and the feedwater inlet valve regulation are also taken into account.

One of the limitations of the model is that it does not treat control rod motions due to use of the point kinetics equation. Another is that it cannot handle accidents situations, because of the assumptions made in the different sub-models. In order to cover these problems it is necessary to use a 3-dimensional reactor model.

2. MODEL OF THE BOILING WATER REACTOR

The model of the boiling water reactor is taken from reference 1 and somewhat modified. It consists of three main parts:

1) The neutron kinetics model,
2) The fuel dynamic and heat transfer model,
3) The hydrodynamic model.

2.1. The Neutron Kinetics Model

The neutron kinetics model is based on "point kinetics", i.e. it is assumed that the power density N(t, k) is separable in space and time

$$N(t, k) = \Phi(t) \cdot P(k)$$

where $\Phi(t)$ is the total nuclear power and P(k) is an axial power distribution parameter. The number of delayed neutron groups taken into account is six. Assuming this "point model", the total nuclear power can be expressed as

$$\frac{d\Phi}{dt} = \frac{\rho_{ex} - \beta}{l} \Phi + \sum_{i=1}^{6} \lambda_i C_i$$

$$\frac{dC_i}{dt} = \frac{\beta_i}{l} \Phi - \lambda_i C_i \qquad (i = 1, 2, \ldots 6)$$

$$\beta = \sum_{i=1}^{6} \beta_i$$

where

C_i is the precursor density of the i'th group

λ_i is the decay constant of the i'th group

β_i is the delayed neutron fraction of the i'th group

ρ_{ex} is the excess reactivity

l is the prompt neutron lifetime.

The coupling between the kinetics model and the hydrodynamic and fuel dynamic model is governed by reactivity feedbacks expressed through the excess reactivity ρ_{ex} by

$$\rho_{ex} = \rho_V + \rho_D + \rho_T$$

where

ρ_V is the void reactivity coefficient

ρ_D is the Doppler reactivity coefficient

ρ_T is the moderator temperature reactivity coefficient.

2.2. The Fuel and Heat Transfer Model

This model describes how the nuclear heat generated by fission in the fuel elements is transferred to the coolant.

The fuel is divided into a number of sections in the axial direction and a number of annular zones of equal area in the radial direction, fig. 2.2.a.

Some assumptions are made before setting up the heat conduction equations and heat transfer equations

1) No axial heat conduction.
2) No heat capacity of gap and canning.
3) The nuclear heat is generated homogeneously over the cross section of the fuel rod except for a fraction δ released promptly into the coolant by γ-radiation.
4) The density and specific heat of the fuel are constants, but heat conductivity depends on the local temperature.
5) The temperature in the middle of each annular zone is equal to the volume average temperature of that zone.
6) The temperature on the boundary between two zones is given from a linear approximation between the centre temperatures.

If the heat conductivity of the fuel λ_F is written as

$$\lambda_F(T_F) = \frac{\varepsilon_1}{1+\varepsilon_2 T_F}$$

where T_F is the fuel temperature on the boundary between two zones and ε_1 and ε_2 are constants, the heat flow $Q_{i,k}$ across the boundary between i and i+1 in the axial section denoted k can be expressed as

$$Q_{i,k} = B_{i+1} \cdot \lambda_i (T_{i,k} - T_{i+1,k}),$$

where $T_{i,k}$ and $T_{i+1,k}$ are the centre temperatures of zones i and i+1 respectively, and B_{i+1} is a constant determined by the radial length of the two zones.

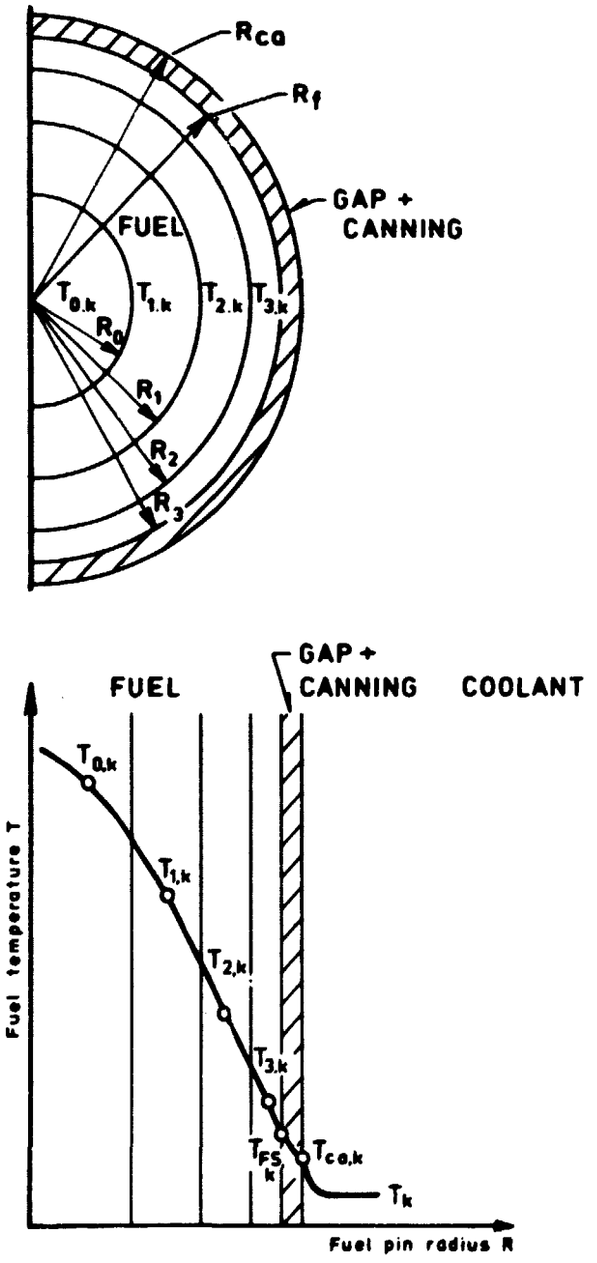

Fig. 2.2.a. At the top: radial division of the fuel into four zones of equal cross section area. Below: radial fuel temperature distribution for axial section k.

If a heat balance is applied to the annular zone number i in the axial section k, the following differential equation can be derived for the fuel temperature in the middle of the zone

$$\frac{dT_{i,k}}{dt} = \frac{1}{H_F}\left[\Phi(t)\, P_k(1-\delta) + A_M(\lambda_{i-1,k}\, b_i(T_{i-1,k} - T_{i,k}) - \lambda_{i,k}\, b_{i+1}\, (T_{i,k} - T_{i+1,k}))\right],$$

where H_F, A_M and b_i are constants determined by geometrical and material parameters, and P_k is an axial power distribution parameter.

Because of the assumption that the gap-canning has no heat capacity, the heat flow from fuel to gap-canning and from gap-canning to coolant is always equal. This heat flow can be written as

$$Q = A_S \cdot K_{g+ca}(T_{FS,k} - T_{ca,k}),$$

where A_S is the heated surface area of each axial section, K_{g+ca} the heat transfer coefficient gap-canning and $T_{FS,k}$ and $T_{ca,k}$, the fuel surface temperature and the canning surface temperature respectively, both in axial section k.

If the coolant outside the canning is boiling, the heat transfer to the coolant is governed by the Jens-Lottes' correlation

$$Q = A_S\left[K_B\,(T_{ca,k} - T_{s,k})\right]^4$$

where

$$K_B = 1.266\, e^{1.61 \cdot 10^{-7} \cdot p}, \qquad (p = \text{pressure } [N/m^2])$$

and $T_{s,k}$ is the saturation temperature of the coolant in section k.

If the coolant outside the canning is in a single-phase state, the heat transfer is determined by the Colburn correlation

$$Q = A_S \cdot K_{NB}(T_{ca,k} - T_k)$$

where

$$K_{NB} = 0.023\, \frac{(\rho_f c_{f,k})^{0.8} \cdot C_p^{0.4} \cdot \lambda_f^{0.6}}{D_C^{0.2} + \mu_f^{0.4}}$$

and

ρ_f is the density of the coolant

$c_{f,k}$ is the velocity of the coolant in section k

C_p is the heat capacity of the coolant

λ_f is the heat conductivity of the coolant

D_C is the hydraulic diameter of the coolant

μ_f is the viscosity of the coolant, and

T_k is the temperature of the coolant in section k.

In order to determine whether boiling heat transfer or non-boiling heat transfer occurs, the correlation that gives the lowest canning temperature is chosen.

The fuel surface temperature $T_{FS,k}$ is calculated by a linear approximation between the centre temperature of the annular zone of the fuel containing the fuel surface and an artificial zone of the same area outside the fuel surface. The centre temperature of this artificial $T_{M,k}$ is determined by iteration, illustrated in fig. 2.2.b.

After this iteration procedure the heat transfer to the coolant can be finally calculated.

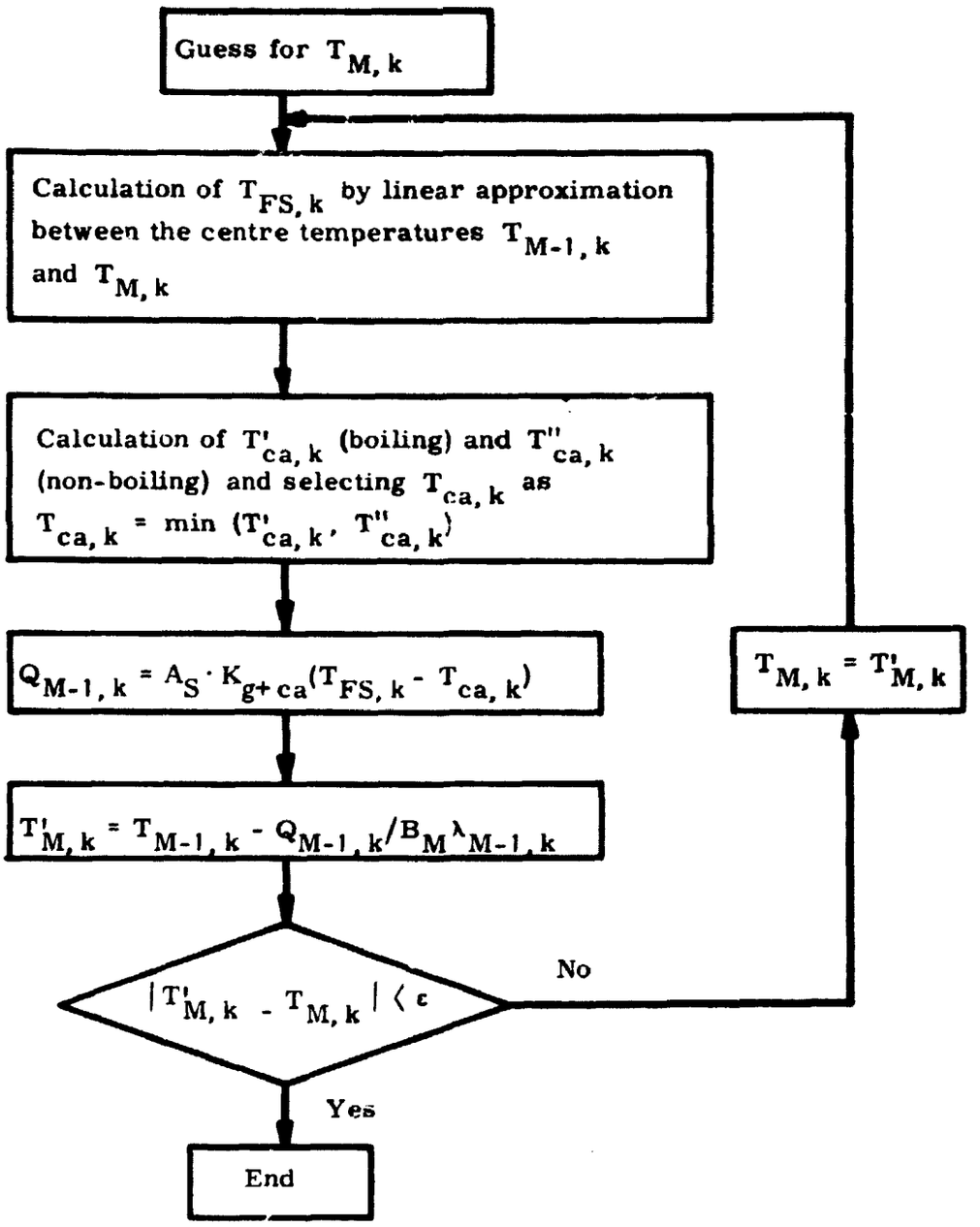

Fig. 2.2.b. Flow chart for the calculation of $T_{M,k}$, the centre temperature of an artificial zone outside the fuel surface. $M = N_a + 1$ where N_a is the number of annular fuel zones.

2.3. The Hydrodynamic Model

The hydrodynamic loop is treated one-dimensionally in space with the division into sections shown in fig. 2.3.a. In order to determine the conditions of the loop, the laws of conservation of mass, energy and momentum

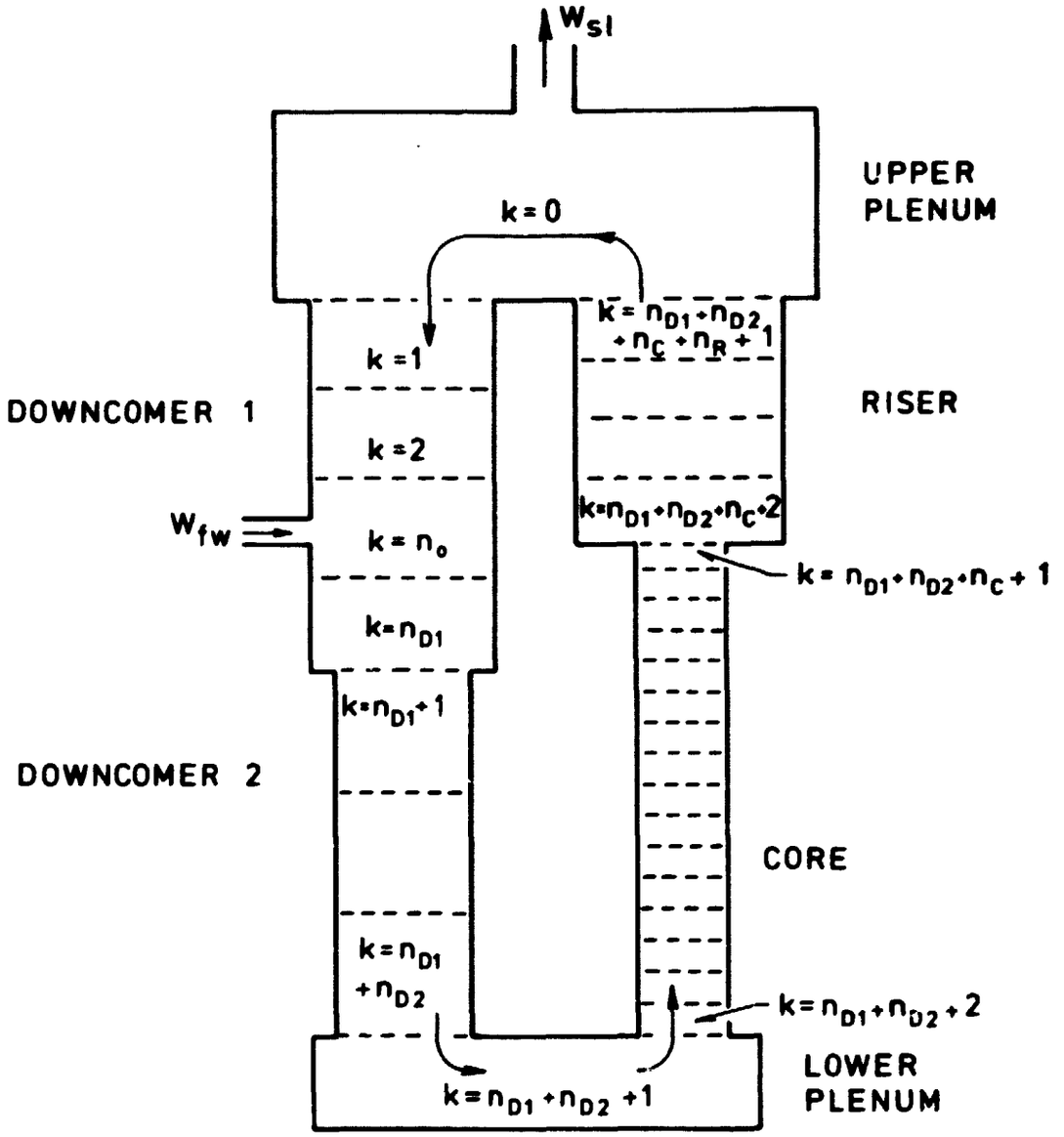

$n_{D1} < 10$: number of axial sections in downcomer 1
$n_{D2} < 10$: number of axial sections in downcomer 2
$n_C < 40$: number of axial sections in core
$n_R < 20$: number of axial sections in riser
n_0 : axial section number where feedwater is returned

Fig. 2.3.a. Division of the hydrodynamic loop into sections.

are set up for each section. In sections with both water and steam present, equations describing the transfer of mass and energy between the two phases are necessary.

2.3.1. The Transfer of Mass and Energy

The transfer of mass and energy between the two phases is governed by two vapour-producing terms, the "surface" term and the "bulk" term. The surface term expresses the steam generated at the surface of the fuel where the water is in contact with a wall at a temperature above the saturation temperature; this term is never negative. The bulk term expresses the flashing and the condensation of water and steam away from the heated surface; thus it can both be positive and negative.

In the model it is assumed that these two terms, Φ_{SF} and Φ_{B}, can be expressed as

$$\Phi_{SF} = \frac{Q(1-\delta)}{h_{fg} + C_p(T_g-T_f)\frac{\rho_f}{\rho_g} + (T_{ca}-T_g)\left(\frac{\rho_f}{\rho_f} - 1\right)\frac{C_p}{2}}$$

where

h_{fg} is the heat of evaporation

C_p if the specific heat of water at constant pressure

T_g and T_f are the temperatures of steam and bulk fluid respectively

ρ_g and ρ_f are the densities of steam and water

and

$$\Phi_B = \frac{1}{h_{fg}} \left[R_o + R_1 \cdot \alpha(1-\alpha)\right] \left[(T_f-T_g) + \varkappa \left|T_f-T_g\right|\right]$$

where

$\varkappa$, R_o and R_1 are input constants, $0 \leq \varkappa \leq 1$

α is the void content.

The physical meaning of the term $R_o + R_1 \cdot \alpha(1-\alpha)$ is the rate of heat transport between the two phases corresponding to complete thermal insulation, if the value of the term is zero, and to thermal equilibrium reached infinitely rapidly, if the value is infinite.

Finally the surface term and bulk term are combined to one given by

$$\Phi_k = A_{H,k} \Phi_{SF,k} + V_k \cdot \Phi_{B,k}$$

and calculated for each section; $A_{H,k}$ is the area of the heated surface in section k, and V_k is the volume of section k.

2.3.2. The Mass Balance for the Two Phases

If M_g and M_f are the masses of steam and water, respectively, in a section with volume V, the mass balance for steam can be expressed as

$$\frac{dM_g}{dt} = \dot{m}_{g,i} - \dot{m}_{g,o} + \Phi$$

where $\dot{m}_{g,i}$ is the mass flow rate of steam at the inlet to the section, $\dot{m}_{g,o}$ the mass flow rate of steam at the outlet of the section, and Φ the total mass transfer rate given by the expression derived above.

In a similar way, the mass balance for the fluid phase can be written as

$$\frac{dM_f}{dt} = \dot{m}_{f,i} - \dot{m}_{f,o} - \Phi ,$$

where $\dot{m}_{f,i}$ is the mass flow rate of water at the inlet to the section, and $\dot{m}_{f,o}$ the corresponding quantity at the outlet. By introducing the volume flow W,

$$W = W_f + W_g = \frac{\dot{m}_f}{\rho_f} + \frac{\dot{m}_g}{\rho_g}$$

and the fact that

$$V = \frac{M_g}{\rho_g} + \frac{M_f}{\rho_f} ,$$

the following equation can be derived under the assumption of no local pressure dependence

$$W_o = W_i + \gamma \cdot \Phi + \eta \cdot \frac{dp}{dt}$$

where

$$\gamma = \frac{1}{\rho_g} - \frac{1}{\rho_f}$$

$$\eta = - M_g \frac{d}{dp}\left(\frac{1}{\rho_g}\right) - M_f \frac{d}{dp}\left(\frac{1}{\rho_f}\right)$$

and W_o, W_i are the total volume flow at outlet and inlet respectively.

Applying the derived equation to the whole hydraulic loop gives the following equation for the reactor system pressure

$$\frac{dp}{dt} = (W_{fw} - W_{sl} + \gamma \Phi_{TOT}) / \eta_{TOT}$$

under the assumption that the densities of water and steam ρ_f and ρ_f only depend on the system pressure p. W_{fW} is the inlet volume flow of feedwater W_{sl} is the outlet volume flow of steam from the reactor, Φ_{TOT} is the total volume production of steam, and η_{TOT} the total compressibility of the steam and water obtained by summing η.

2.3.3. The Equation of Conservation of Energy

Only one energy balance equation is applied, i.e. the term describing the energy transfer between the two phases is cancelled out. With the specific internal energy for steam and water called e_g and e_f, the internal energy of a section with the volume V can be expressed as

$$E = M_g e_g + M_f e_f .$$

The energy balance equation for this section becomes

$$\frac{dE}{dt} = Q + W_{E,i} - W_{E,o} ,$$

where Q is the heat rate supplied to the section, $W_{E,i}$ the inlet flow of energy, and $W_{E,o}$ the outlet flow expressed as

$$W_E = \dot{m}_g \left(e_g + \frac{p}{\rho_g}\right) + \dot{m}_f \left(e_f + \frac{p}{\rho_f}\right) = \dot{m}_g \cdot h_g + \dot{m}_f \cdot h_f ,$$

where h_g and h_f are the specific enthalpies of steam and water respectively.

With the assumption that the steam is always in a saturated condition, the specific internal energy of the steam is only a function of the pressure. The water temperature T_f can thus be found from

$$T_f = T_f(e_f, p) ,$$

with

$$e_f = \frac{E - M_g\, e_g(p)}{M_f} .$$

Finally, we introduce a relation between the velocity of the steam c_g and the velocity of the water c_f through a slip parameter S

$$c_g = S \cdot c_f + c^o ,$$

where c^o is the rise velocity of steam bubbles in quiescent water. The slip parameter S is given by the Bankoff correlation

$$S = S_1 + S_2\, \alpha^{1.8} ,$$

where S_1 and S_2 are input constants and α the void content in the section considered.

The equations necessary to describe the dynamic conditions for every section along the flow path have now been presented and a solution can be obtained, from the flowchart of the hydraulic loop on the next page.

The calculation starts in the first section of the downcomer 1, see fig. 2.3.a, and proceeds around the loop until the last section in the riser. However, from the flow chart of the hydraulic loop it appears that the inlet conditions of the first section of downcomer 1, corresponding to k = 1, cannot be determined from the derived equations. The equation of momentum can be applied to solve this problem.

2.3.4. Determination of the Inlet Conditions of Downcomer 1 from the Momentum Equation

The momentum equation for an infinitesimal part of the flow path along z can be written as

$$\frac{\partial i}{\partial t} + \frac{\partial U}{\partial z} = - \frac{\partial p}{\partial z} + g \cdot \frac{M}{A} - f ,$$

where i is the momentum, U is the momentum flow, p is the static pressure, $g \cdot \frac{M}{A}$ is the weight of the steam-water mixture and f the friction.

Integration of this equation around the flow loop gives

$$\frac{dI}{dt} = D - F - L$$

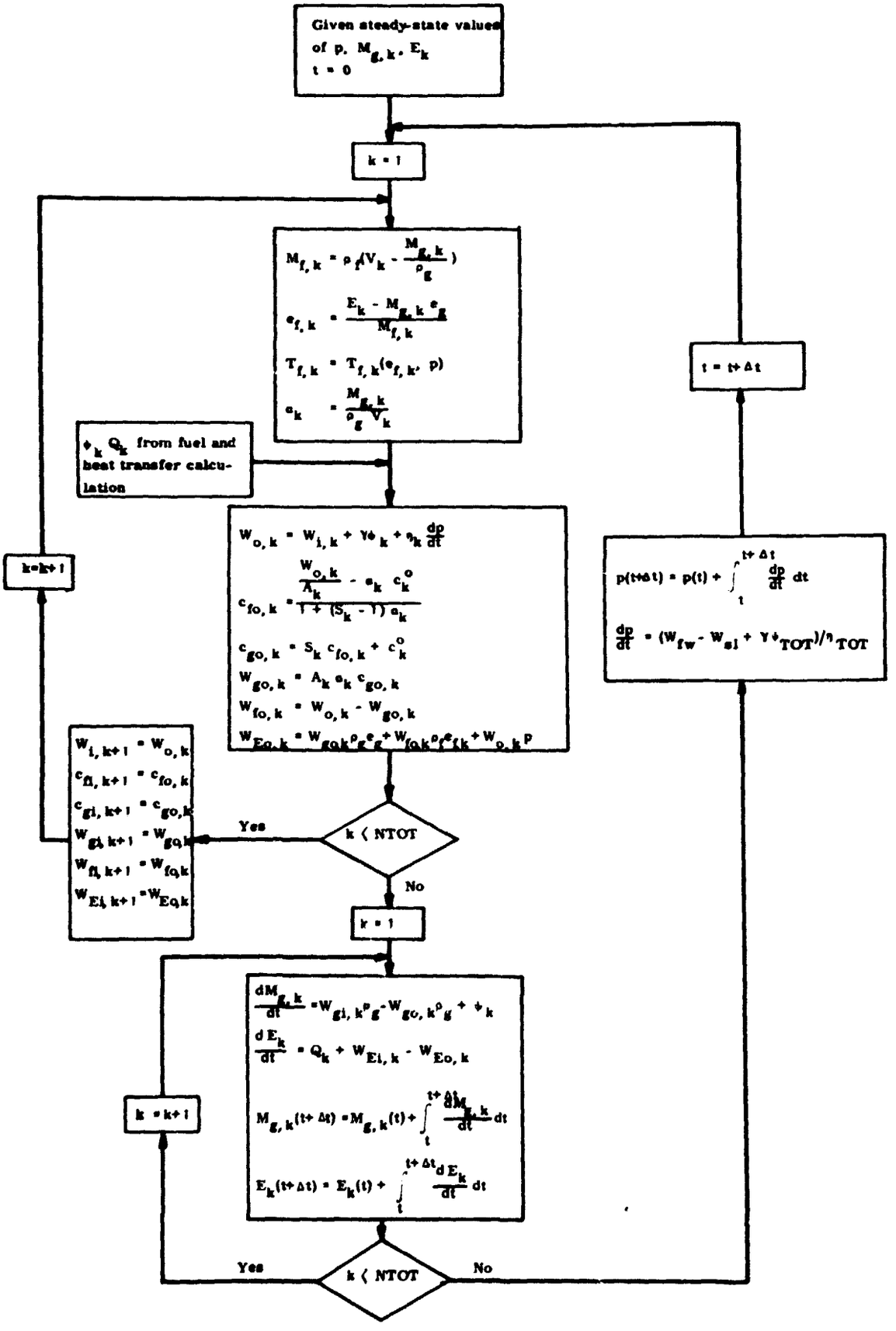

Fig. 2.3.3.a. Flow chart of the hydraulic loop.

where the driving force D is calculated as

$$D = \sum_{k=1}^{NTOT} g_k \frac{M_k}{A_k} \Delta z_k + \Delta p_{pump}$$

with the summation term expressing the natural circulation from the gravity force and Δp_{pump} expressing the forced circulation from the circulation pump placed in one of the downcomers. The friction term F is given by

$$F = \sum_{k=1}^{NTOT} f_k \cdot R_k \frac{|\dot{m}_{g,k} + \dot{m}_{f,k}| (\dot{m}_{g,k} + \dot{m}_{f,k})}{\rho_f \cdot A_k^2}$$

with $\dot{m}_g$ and $\dot{m}_f$ as mass flow rate of steam and water respectively, A_k the flow area, f_k the single phase friction factor, and R_k the two-phase friction multiplier given as

$$f_k = \frac{0.184}{2 \cdot D_k \cdot Re_k^{0.2}}$$

$$R_k = 1 + 2400 \left(\frac{x_k}{p}\right)^{0.96}$$

where D_k is the hydraulic diameter, Re_k is the Reynold's number and x_k is the quality.

Finally the term L expresses the losses caused by pressure drops at singularities and the momentum flow losses at area changes

$$L = - \sum_{\text{singularities}} \frac{1}{2} \cdot L_{k,k+1} \cdot U_{o,k} + \sum_{k=1}^{NTOT} (U_{o,k} - U_{i,k+1})$$

$$U_{o,k} = (|\dot{m}_{g,k}| c_{g,k} + |\dot{m}_{f,k}| c_{f,k})/A_k$$

$$U_{i,k+1} = U_{o,k} \cdot \left(\frac{A_k}{A_{k+1}}\right)^2$$

where $L_{k,k+1}$ are input constants and $c_{g,k}$ and $c_{f,k}$ are steam and water velocities at the exit of section k. The total integrated momentum per unit

area becomes

$$I = \sum_{k=o}^{NTOT} ((1 - a_k)\rho_f c_{f,k} - a_k \rho_g c_{g,k}) \Delta z_k ,$$

or expressed by the volume flow W_k and slip factor S_k

$$I = \sum_{k=o}^{NTOT} \frac{W_k}{A_k} (\rho_f + (\rho_g - \rho_r) B_k - c_k^o a_k (\rho_f - \rho_g) (1 - B_k))$$

where

$$B_k = \frac{S_k a_k}{1 + (S_k - 1) a_k} .$$

From the earlier derived expression for the volume flow

$$W_{o,k} = W_{i,k} + \gamma_k \phi_k + \eta_k \cdot \frac{dp}{dt} ,$$

we can calculate

$$W_{o,k} = W_{i,1} + \sum_{i=1}^{k} (\gamma_i \phi_i + \eta_i \frac{dp}{dt} + \delta_i W_{fw})$$

$$\delta_i = \begin{cases} 1 & \text{for } i = i_{fw} = \text{number of section of feedwater inlet} \\ 0 & \text{for } i \neq i_{fw} \end{cases}$$

where $W_{i,1}$ is the inlet volume flow to the downcomer 1. If $W_{o,k} = W_k$ is inserted into the expression for the integrated momentum, the following expression can be derived

$$W_{i,1} = \frac{I - \sum_{k=1}^{NTOT} \{C_k [\sum_{i=1}^{k} (\gamma_i \phi_i + \eta_i \frac{dp}{dt} + \delta_i W_{fw})] - c_k^o D_k\}}{\sum_{k=1}^{NTOT} C_k}$$

where

$$C_k = (\rho_f + (\rho_g - \rho_f) B_k) \frac{\Delta z_k}{A_k}$$

$$D_k = a_k(\rho_f - \rho_g)(1 - B_k) \cdot \Delta z_k .$$

The derived expression for the inlet volume flow to the downcomer 1, together with

$$I(t + \Delta t) = I(t) + \int_t^{t + \Delta t} (D - F - L)dt ,$$

thus close the set of equations necessary to find the state of every section in the hydraulic loop as time proceeds.

2.4. The Steady-State Solution

To obtain a steady-state solution for the neutron kinetic model and the fuel model, the time derivatives are set equal to zero, and the system of algebraic equations is solved. The hydrodynamic model follows another procedure, where the differential equations are integrated to obtain a steady-state solution. First, it is assumed that the void content in every section is zero and that the temperatures are equal to the saturation temperature corresponding to the system pressure. Assuming the inlet velocity to the core to be 1 m/s, the momentum I is calculated and kept constant. Then the power is increased linearly from zero to the nominal value, with the feed-water inlet flow equal to the steam load and this again equal to the steam generated in the core, still with momentum I kept constant. When nominal power is reached, the differential equation of momentum is introduced and the whole set of equations is integrated until the different variables become constant and the time derivatives zero.

This method of obtaining a steady-state solution is rather time-consuming; its advantage lies in the fact that there is no need for additional programming to solve algebraic equations.

The integration is done by the simple Euler method given as

$$y(t + \Delta t) = y(t) + \left(\frac{dy}{dt}\right)_t \Delta t$$

with a truncation error of

$$\frac{1}{2}(\Delta t)^2 \cdot \left(\frac{dy^2}{dt^2}\right)_{t_m} \quad ; \qquad t \leq t_m \leq t + \Delta t.$$

Fig. 2.4.a finally shows a diagram of the calculation procedure for the whole reactor model. The steam load is lead to the turbine model (described later), and then returns to the reactor as water via the feedwater cascade model (also presented later).

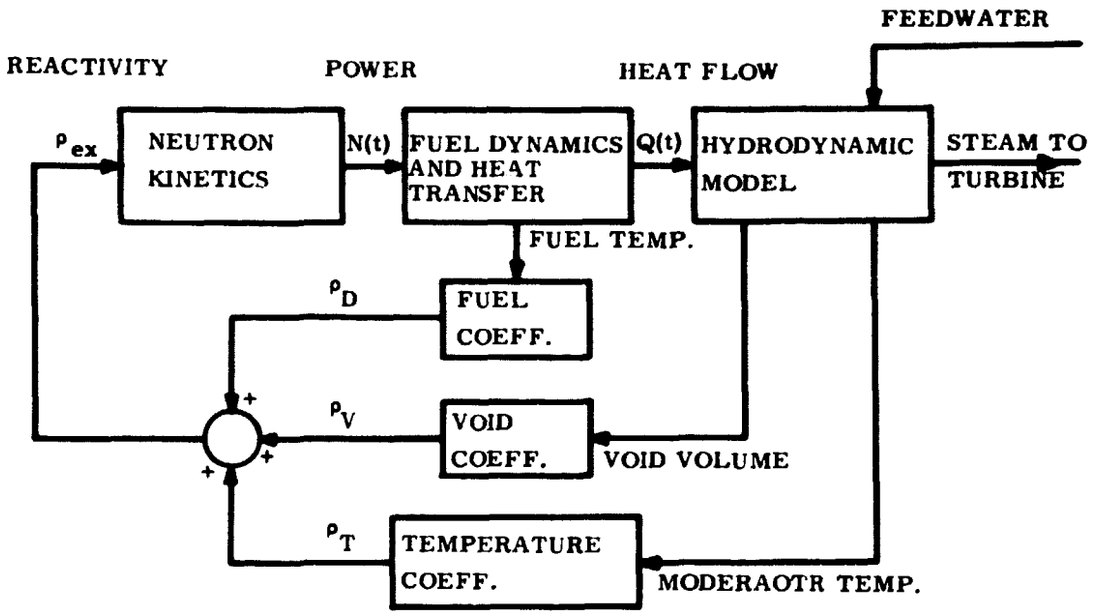

Fig. 2.4.a. Flow chart for the calculation of the reactor model.

3. MODEL OF THE TURBINE

The dynamic model of the turbine described here is based on the steady-state model developed in part I, where each nozzle row and blade row is treated in some detail. The approach used in the dynamic model is shown in fig. 3.a.

This shows a turbine with 9 stages and 2 feedwater extraction lines placed at the outlet of stage number 3 and at the outlet of stage number 6. In the steady-state model the continuity and the energy equations were set up for each nozzle row and blade row; here these equations will be used only for the extraction rooms 2 and 3. The volume of room 2, e.g., is increased by the volume of the three first stages upstream, room 3 is increased by

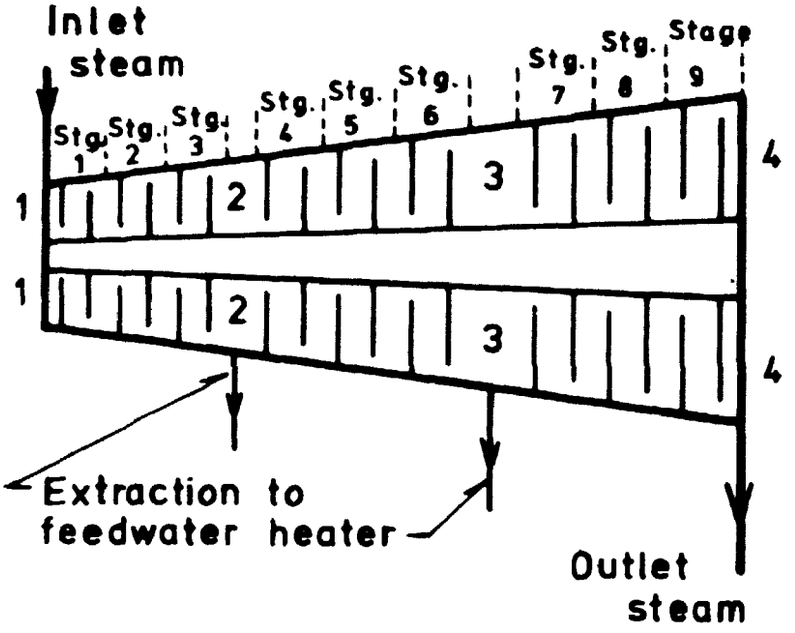

Fig. 3.a. Turbine with 9 stages and 2 extraction lines to feedwater heaters.

the volume of the stages between rooms 2 and 3, etc. This means that the time-lag of the flow through the turbine is assumed to be caused by the extraction room to the feedwater heaters and the flow between these rooms is thus always steady-state.

3.1. Determination of the Flow between the Extraction Rooms

The continuity equation at the outlet of each stage can be written as

$$\dot{m} = \frac{A_2 \cdot c_{2n}}{v_2}$$

where A_2 is the flow area at the exit of the stage, c_{2n} is the velocity component perpendicular to this area, and v_2 is the specific volume of the steam-water mixture. By introducing a quantity μ

$$\mu = \frac{c_{2n}}{\sqrt{2\Delta h_s}}$$

where Δh_s is the isentropic enthalpy drop across the stage, we get

$$\frac{\dot{m}^2}{2\mu^2 A_2^2} = \frac{\Delta h_s}{v_2^2} . \qquad (3.1.1)$$

By combining the first and second laws of thermodynamics, we can derive for an infinitesimal change of enthalpy

$$dh = T\,ds + v\,dp,$$

where T is the temperature, s is the entropy, and p is the pressure. Applying this equation to an isentropic process gives

$$dh_s = v\,dp.$$

Introducing this in equation (3.1.1), and assuming Δh_s to be small and $v_2 = v$, gives

$$\frac{\dot{m}^2}{2\mu^2 A_2^2} = \frac{\Delta p_2}{v_2} . \qquad (3.1.2)$$

We now assume that the expansion through a turbine stage can be represented by a polytropic exponent n in the following way

$$v_2 = v_o \cdot \left(\frac{p_o}{p_2}\right)^{1/n} ,$$

where the index o refers to the inlet of the stage and 2 refers to the outlet of the stage. By introducing this in the equation (3.1.2), we get

$$\frac{\dot{m}^2}{2\mu^2 A_2^2} = \frac{1}{v_o}\left(\frac{p_2}{p_o}\right)^{1/n} \Delta p_2 .$$

This equation is valid for every stage and by summing this over a number of stages, N, we get

$$\dot{m}^2 \sum_{i=1}^{N} \frac{1}{2\mu_i^2 A_{2i}^2} = \frac{1}{v_o (p_o)^{1/n}} \cdot \sum_{i=1}^{N} (p_{2i})^{1/n}\, \Delta p_{2i} .$$

Assuming N to be large and using the approximation

$$\sum_{i=1}^{N} (p_{2i})^{1/n} \Delta p_{2i} \approx \int_{p_N}^{p_o} p^{1/n}\, dp = \frac{n}{n+1}\left[p_o^{\frac{n+1}{n}} - p_N^{\frac{n+1}{n}} \right],$$

where p_o is the pressure at the inlet to the first stage, and p_N is the pressure at the outlet of stage number N, we finally get

$$\dot{m}^2 \sum_{i=1}^{N} \frac{1}{2\mu_i^2 A_{2i}^2} = \frac{1}{v_o}\frac{n}{n+1}\left[p_o - p_N^{\frac{n+1}{n}} \cdot p_o^{-\frac{1}{n}} \right] = \frac{p_o}{v_o}\frac{n}{n+1}\left[1 - \left(\frac{p_N}{p_o}\right)^{\frac{n+1}{n}} \right]$$

From reference 2 it is known that μ_i has almost the same value for every stage and that this value can be considered as a constant during varying load conditions. If we indicate the values at nominal conditions by the index zero, we get the following expression for the mass flow rate under varying load conditions

$$\dot{m} = \dot{m}_o \sqrt{\frac{p_o v_{oo}}{p_{oo} v_o}} \sqrt{\frac{1 - (p_N/p_o)^{\frac{n+1}{n}}}{1 - (p_{No}/p_{oo})^{\frac{n+1}{n}}}} \,. \qquad (3.1.3)$$

The values of the nominal quantities $\dot{m}_o$, p_{oo}, p_{No}, v_{oo} are determined from the steady-state calculation with "TURBPLANT" (part I) as well as the value of the polytropic exponent n. This exponent fulfils the relation $1.3 > n > 1.0$ depending on where the expansion takes place in the Mollier diagram.

3.2. Determination of the Pressure, the Enthalpy and the Entropy for the Extraction Rooms

It is now assumed that the state of the steam-water mixture in the extraction rooms is always at thermal equilibrium. A mass balance equation and an energy balance equation are then set up for these rooms. With room 2 in fig. 3.a as example, these equations can be written as

$$\frac{dM_2}{dt} = \dot{m}_{2i} - \dot{m}_{2o}$$

and

$$\frac{dh_{2o}\, M_2}{dt} = h_{2i} \cdot \dot{m}_{2i} - h_{2o} \cdot \dot{m}_{2o} \,,$$

where M_2 is the total mass of the steam-water mixture in room 2, $\dot{m}_{2i}$ is the inlet mass flow rate and $\dot{m}_{2o}$ is the outlet flow rate, h_{2i} is the specific enthalpy of the inlet mass flow, and h_{2o} is the specific enthalpy of the outlet mass flow equal to the specific enthalpy of the mixture in room 2.

$\dot{m}_{2i}$ is given by the expression (3.1.3), here written as

$$\dot{m}_{2i} = \dot{m}_{2io}\, E(v_1, \frac{p_2}{p_1})$$

where

$$E(v_1, \frac{p_2}{p_1}) = \sqrt{\frac{p_1 v_{1o}}{p_{1o} v_1}} \sqrt{\frac{1 - (p_2/p_1)^{\frac{n+1}{n}}}{1 - (p_{2o}/p_{1o})^{\frac{n+1}{n}}}} \,.$$

$\dot{m}_{2o}$ is given as the sum of two terms. The first term is the flow to the next extraction room given by $m_{3io}\, E(v_2, p_3/p_2)$ and the second term expresses the mass flow rate to the feedwater heater, given as

$$\dot{m}_{FW} = A \cdot \left[\frac{n}{n-1} \left(\frac{p_2}{v_2}\right) \left(\left(\frac{p_{FW}}{p_2}\right)^{2/n} - \left(\frac{p_{FW}}{p_2}\right)^{\frac{n+1}{n}} \right) \right]^{1/2} ,$$

where p_{FW} is the pressure in the feedwater heater; this expression is taken from reference 4, and is equivalent to expression (3.1.3) for a single stage. A is a constant proportional to the flow area of the extraction line and n is the polytropic exponent; they are both calculated from the steady-state solution described in part I of this report.

In order to calculate the inlet enthalpy h_{2i}, the inlet steam quality x_{2i} is first determined by applying the polytropic relation

$$v_{2i} = v_1 \left(\frac{p_1}{p_2}\right)^{1/n}$$

and the expression

$$x_{2i} = \frac{v_{2i} - v_f(p_2)}{v_g(p_2) - v_f(p_2)} .$$

The inlet enthalpy can then be calculated from

$$h_{2i} = h_f(p_2) + x_{2i}(h_g(p_2) - h_f(p_2)) .$$

In the above-mentioned expressions, $v_f(p_2)$ and $v_g(p_2)$ are the specific volumes of water and steam respectively and $h_f(p_2)$, $h_g(p_2)$ the specific enthalpies of water and steam, all quantities being evaluated at the saturation pressure p_2.

By solving the two coupled differential equations for mass and energy derived above, new values of the mass content and the energy content of the extraction room are obtained for every time step. The specific volume and the specific enthalpy of the steam-water mixture in the extraction room can then be calculated if the volume V_2 of the room is known.

In order to determine the pressure of the extraction room at every time step, it is necessary to introduce two new equations. With both the water phase and the steam phase present, corresponding to the extraction room located below the saturation line in the Mollier diagram, (see part I), these equations for the specific volume and the specific enthalpy can be written as

$$v_2 = v_f(p_2) + x_2 \cdot (v_g(p_2) - v_f(p_2))$$

$$h_{2o} = h_f(p_2) + x_2 \cdot (h_g(p_2) - h_f(p_2))$$

where $v_2 = V_2/M_2$ and x_2 is the steam quality of the extraction room.

We now have two equations with two unknowns, p_2 and x_2, which can be solved. This must be done by iteration because v_f, v_g, h_f and h_g are represented in the model as seventh order polynomials in the saturation pressure. Thus, after determining the pressure p_2 at the new time step, the entropy of the extraction room can be finally calculated from

$$s_2 = s_f(p_2) + x_2 \cdot ((s_g(p_2) - s_f(p_2)))$$

where s_f and s_g are the entropies of water and steam respectively.

If the state of the extraction room is supersaturated, the equations determining the pressure are reduced to one

$$v_2 = \text{VSUP}(p_2, h_{2o}) .$$

Since the function VSUP(p, h) is represented in the model as third-order polynomials in the variable pressure and enthalpy, iteration is also necessary in this case to determine the pressure p_2 from the known values of v_2 and h_{2o}; the entropy is calculated from

$$s_2 = \text{SSUP}(p_2, v_2).$$

3.3. Flow and Power Calculation for the Whole Turbine

The calculation procedure mentioned above is now used for every feed-water extraction room along the turbine. Assuming the inlet conditions of the turbine to be known, the mass flow rates in and out of these rooms can be determined together with the pressure, enthalpy and entropy of these rooms as time proceeds. This means that a Mollier diagram of the expansion through the turbine can be calculated for every time step and the flow and energy conditions of the turbine are thus fully determined.

Still referring to fig. 3.a, the power delivered to the turbine blades can be calculated as

$$N = \dot{m}_{2i}(h_{1o} - h_{2i}) + \dot{m}_{3i}(h_{2o} - h_{3i}) + \dot{m}_{4i}(h_{3o} - h_{4i}) .$$

Finally it must be mentioned that the integration of the mass equation and the energy equation, (3, 2, 1) and (3. 2. 2), has caused much trouble due to the very high mass flow rates in and out of the extraction rooms compared with the rather small mass content of the rooms. Among several integration methods, the modified Euler method, ref. 5, was found to be the best. It is defined as

$$y_p(t_o + \Delta t) = y(t_o) + \left(\frac{dy}{dt}\right)_{t_o} \Delta t$$

$$y_c(t_o + \Delta t) = y(t_o) + \left[\left(\frac{dy}{dt}\right)_{t_o} + \left(\frac{dy_p}{dt}\right)_{t_o+\Delta t}\right]\frac{\Delta t}{2}$$

with a truncation error of

$$\frac{5}{12}(\Delta t)^3 \cdot \left(\frac{dy_c^3}{dt^3}\right)_{t_m} \quad ; \qquad t \leq t_m \leq t + \Delta t$$

where y_p is the predictor given by the simple Euler method and y_c is the corrector representing the modified Euler method. Even with this method, time steps of a few milliseconds only are needed to avoid numerical instabilities.

4. MODEL OF THE COMBINED MOISTURE SEPARATOR-REHEATER

As described in part I, the purpose of the moisture separator-reheater is partly to improve the efficiency of the plant and partly to avoid erosion of the blades in the last stages of the low-pressure turbine by increasing the steam quality at the outlet of the low-pressure turbine.

In fig. 4.a is shown a sketch of the combined moisture separator-reheater model.

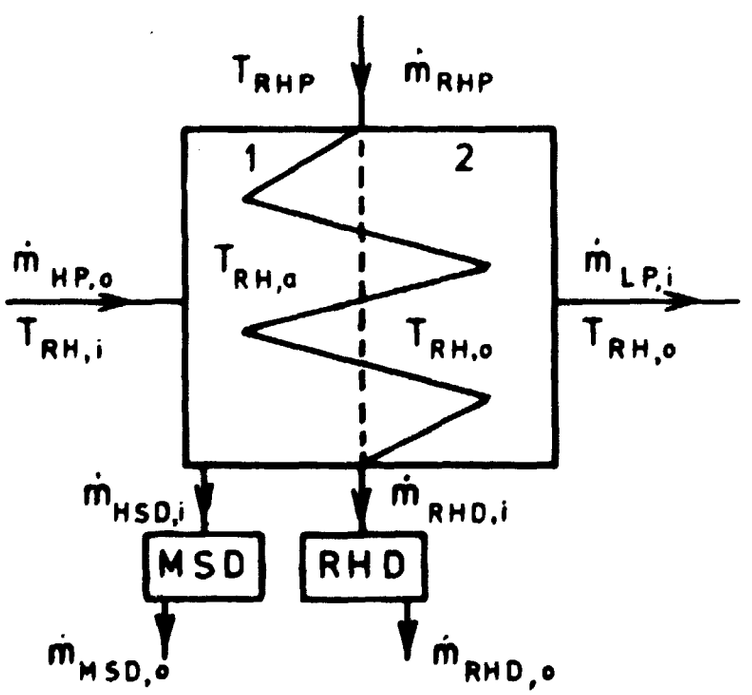

Fig. 4.a. Sketch of the combined moisture separator-reheater model with two drainage tanks.

The primary steam from the reactor $\dot{m}_{RHP}$ enters the bundles of U-tubes and condenses, giving up its heat of evaporation to the secondary steam coming from the high-pressure turbine and flowing on the shell side of the reheater. The condensed water from the primary steam $\dot{m}_{RHD,i}$ enters a drainage tank RHD, from where it is led to a feedwater heater via a level regulation valve. The secondary steam from the high pressure turbine $\dot{m}_{HP,o}$ first flows through some chevrons. where most of the water is separated out, before it flows across the heating tube bundles. The drain from the moisture separator $\dot{m}_{MSD,i}$ enters a drainage tank MSD, and via a level regulation valve it is led to one of the feedwater heaters. The secondary side or shell side of the reheater is divided into two parts, rooms 1 and 2, with equal volume. The temperature in room 1 is $T_{RH,a}$, an average temperature, and in room 2 $T_{RH,o}$, the outlet temperature.

4.1. Determination of the Pressure on the Secondary Side of the Reheater

The pressure in the two rooms is assumed to be the same p_{RHS}; it is determined by a mass balance equation

$$\frac{dM_{RHS}}{dt} = \dot{m}_{HP,o} - \dot{m}_{MSD,i} - \dot{m}_{LP,i}$$

where M_{RHS} is the total mass of steam in the two rooms. Referring to fig. 4.1.a, the other terms in the equation can be derived in the following way

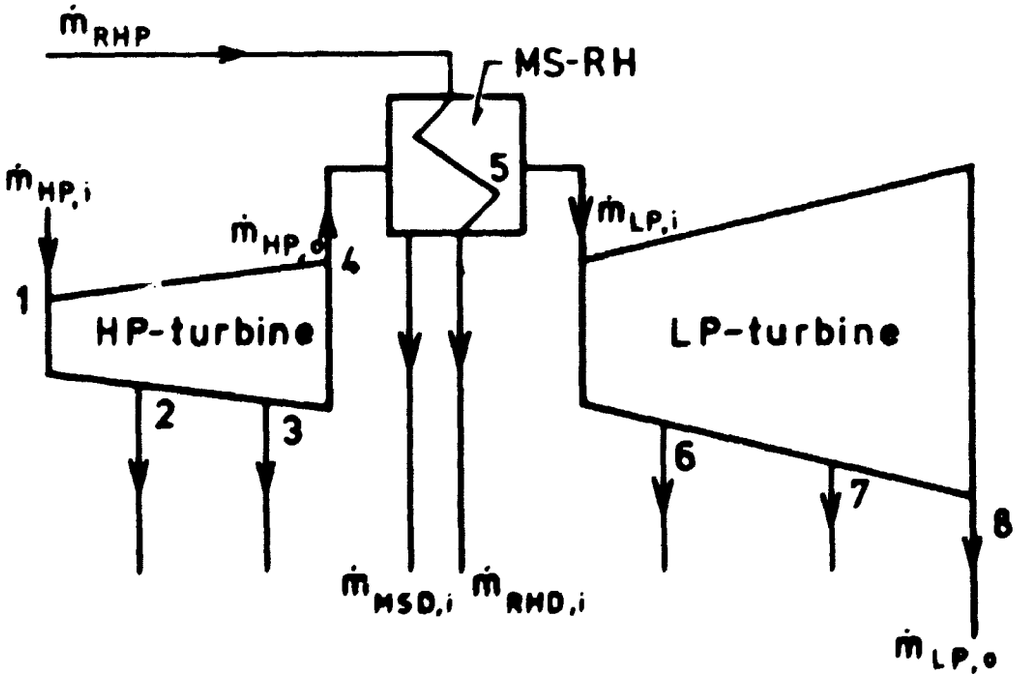

Fig. 4.1.a. Supporting sketch for deriving the mass balance equation for the secondary side of the moisture separator-reheater.

The mass flow rate of steam from the high-pressure turbine $\dot{m}_{HP,o}$, is calculated as

$$\dot{m}_{HP,o} = \dot{m}_{4io} \cdot E(v_3, \frac{p_4}{p_3}) .$$

The mass flow rate of drain from the moisture separator $\dot{m}_{MSD,i}$ is calculated as

$$\dot{m}_{MSD,i} = \dot{m}_{HP,o} \cdot (1 - x_{HP,o}) \cdot \eta_{MS} ,$$

where $x_{HP,o}$ is the steam quality at outlet of the high-pressure turbine and η_{MS} is an efficiency parameter for the water separation ability of the moisture separator. Finally, the mass flow rate at inlet to the low-pressure turbine $\dot{m}_{LP,i}$ can be calculated as

$$\dot{m}_{LP,i} = \dot{m}_{6io} E(v_5, \frac{p_6}{p_5}) ,$$

where p_5 is the reheater pressure p_{RHS}, and v_5 is the specific volume of the steam in room 2, fig. 4.a. As discussed in part I, the pressure drop across the moisture separator-reheater is very difficult to determine. On the basis of the results obtained with the steady-state model, it is therefore assumed that, knowing the pressure in the reheater p_{RHS}, the pressure at the outlet of the high-pressure turbine p_4 can be calculated as

$$p_4 = \frac{p_{RHS}}{0.9} ,$$

corresponding to a pressure drop of 10% of pressure at the outlet of the high-pressure turbine.

If we know the temperature of the steam in rooms 1 and 2, $T_{RH,a}$ and $T_{RH,o}$ we can finally calculate the reheater pressure at a new time step by iteration of the equation

$$M_{RHS} = \frac{V_1}{v(p, T_{RH,a})} + \frac{V_2}{v(p, T_{RH,o})} ,$$

with respect to the pressure p. The function v(p, T) is the specific volume of supersaturated steam at the pressure p and the temperature T; it is represented in the model as a polynomial in two variables. V_1 and V_2 are the volumes of rooms 1 and 2.

4.2. Determination of the Heat Transfer in the Reheater

Returning to fig. 4.a, a heat balance for room 1 can be written as

$$\frac{dT_{RH,a}}{dt} = \frac{\dot{m}_{RHS}}{M_{RHS1}} (T_{RH,i} - T_{RH,a}) + \frac{(UA)_1}{C_p \cdot M_{RHS1}} \cdot (T_{RHP} - T_{RH,a}) \tag{4.2.1}$$

and for room 2

$$\frac{dT_{RH,o}}{dt} = \frac{\dot{m}_{RHS}}{M_{RHS2}} (T_{RH,a} - T_{RH,o}) + \frac{(UA)_2}{C_p \cdot M_{RHS2}} \cdot (T_{RHP} - T_{RH,o}) \tag{4.2.2}$$

where the mass flow rate on the secondary side is calculated as

$$\dot{m}_{RHS} = \frac{\dot{m}_{HP,o} - \dot{m}_{MSD,i} + \dot{m}_{LP,i}}{2}$$

and the weight of the steam in rooms 1 and 2 as

$$M_{RHS1} = \frac{V_1}{v(p_{RHS}, T_{RH,a})}$$

and

$$M_{RHS2} = \frac{V_2}{v(p_{RHS}, T_{RH,o})} .$$

C_p is the specific heat of the steam at constant pressure and $(UA)_1$ is the product of the heat transfer coefficient U and the area A for room 1; $(UA)_2$ is the same quantity for room 2. T_{RHP} is the temperature of primary steam in the tubes. The rate at which steam condenses in these tubes, $\dot{m}_C$, is given as

$$\dot{m}_C = \frac{(UA)_1}{h_{fg}} (T_{RHP} - T_{RH,a}) + \frac{(UA)_2}{h_{fg}} (T_{RHP} - T_{RH,o}) , \tag{4.2.3}$$

where h_{fg} is the specific heat of evaporation evaluated at the pressure of the primary side p_{RHP}.

If the weight of the steam on the primary side is termed M_{RHP}, a mass balance gives

$$\frac{dM_{RHP}}{dt} = \dot{m}_{RHP} - \dot{m}_C \qquad (4.2.4)$$

where

$$\dot{m}_{RHP} = A\left[\frac{n}{n-1}\left(\frac{p_R}{v_R}\right)\left(\left(\frac{p_{RHP}}{p_R}\right)^{2/n} - \left(\frac{p_{RHP}}{p_R}\right)^{\frac{n+1}{n}}\right)\right]^{1/2} . \qquad (4.2.4a)$$

p_R is the reactor system pressure and v_R the specific volume of steam at the saturation pressure p_R. Assuming saturated conditions on the primary side, the pressure p_{RHP} can thus be determined from

$$p_{RHP} = PSAT(v_p); \qquad v_p = \frac{V_p}{M_{RHP}},$$

where V_p is the volume of the primary side and the function PSAT(v) is the pressure as a function of specific volume at saturated conditions; this function is implemented in the model as a seventh-order polynomial.

Finally, the mass balance and energy balance for the drainage tank RHD can be written as

$$\frac{dM_{RHD}}{dt} = \dot{m}_C - \dot{m}_{RHD,o} \qquad (4.2.5)$$

and

$$\frac{dT_{RHD}}{dt} = \frac{1}{M_{RHD}}\left(\dot{m}_C \cdot T_{RHP} - \dot{m}_{RHD,o} \cdot T_{RHD}\right), \qquad (4.2.6)$$

where M_{RHD} is the mass of the water in the drainage tank and T_{RHD} the temperature. The outlet flow from the drainage tank $\dot{m}_{RHD,o}$ to one of the feedwater heaters is calculated as

$$\dot{m}_{RHD,o} = k\frac{A}{\sqrt{1-A^2}}\sqrt{\frac{2(p_{RHP}-p_{FW})}{v_{RHD}}}$$

which is the flow equation for water passing a valve with area A (ref. 6). k is a constant dependent on the performance of the valve. The regulation

of the water level in the tank by means of this valve will be described later.

The five differential equations (4.2.1), (4.2.2), (4.2.4), (4.2.5) and (4.2.6) can now be solved by using the initial values obtained from the steady-state model. "TURBPLANT" thus calculates the values of $\dot{m}_{RHS}$, $\dot{m}_{C}$, $\dot{m}_{HP,o}$, $\dot{m}_{MSD,i}$, $\dot{m}_{LP,i}$, $T_{RH,i}$, $T_{RH,o}$, T_{RHP}, p_{RMS} and p_{RHP} at nominal conditions and, from the three equations (4.2.1), (4.2.2) and (4.2.3), the initial values of $T_{RH,a}$, $(UA)_1$ and $(UA)_2$ can be determined by setting the time derivatives equal to zero. The values of $(UA)_1$ and $(UA)_2$ thus obtained are then considered as constants during the following dynamic calculation.

Finally it must be mentioned that the matrix exponential method outlined in appendix A is used to solve the above-derived five differential equations. It is a semi-analytical method characterized by a high degree of numerical stability.

4.3. The Equations for the Moisture Separator Drainage Tank

The mass and energy equation of the moisture separator drainage tank shown in fig. 4.a can be written as

$$\frac{dM_{MSD}}{dt} = \dot{m}_{MSD,i} - \dot{m}_{MSD,o}$$

$$\frac{dT_{MSD}}{dt} = \frac{1}{M_{MSD}} (\dot{m}_{MSD,i}\, T_{RH,i} - \dot{m}_{MSD,o}\, T_{MSD})$$

where M_{MSD} is the total mass content of the drainage tank, T_{MSD} is the temperature of the drain, and $\dot{m}_{MSD,o}$ is the mass flow rate through the level regulation valve, located on the drain line to some feedwater heater. This mass flow is calculated from

$$\dot{m}_{MSD,o} = k \frac{A}{\sqrt{1-A^2}} \sqrt{\frac{2(p_{RHS} - p_{FW})}{v_{MSD}}}$$

where v_{MSD} is the specific volume of the water in the tank and A is the area of the valve.

These equations are solved at each time step using the Euler method.

5. MODEL OF THE CONDENSER

The condenser is assumed to be capable of maintaining a constant pressure on the shell side under all circumstances. The drain coming from the last drain cooler in the feedwater heater cascade and the condensate from the low-pressure turbine are assumed to be mixed in a holdup tank described by the two differential equations

$$\frac{dM_H}{dt} = \dot{m}_{LP,o} + \dot{m}_{DC,o} - \dot{m}_{FW}$$

$$\frac{dT_H}{dt} = \frac{1}{M_H}\left(\dot{m}_{LP,o} \cdot T_C + \dot{m}_{DC,o} \cdot T_{DC,o} - \dot{m}_{FW} \cdot T_H\right)$$

where $\dot{m}_{LP,o}$ is the mass flow rate at outlet of the low-pressure turbine, $\dot{m}_{DC,o}$ is the mass flow rate at outlet of the last drain cooler in the feedwater heater cascade, $T_{DC,o}$ is the temperature of this drain, T_C is the temperature on the shell side of the condenser, $\dot{m}_{FW}$ is the mass flow rate of the feedwater, and finally M_H is the weight of the water in the holdup tank and T_H is the temperature of this water, equal to the feedwater temperature at the inlet to the first feedwater heater.

The mass H_M and the temperature T_H are calculated at each time step using Euler's method.

6. MODEL OF A FEEDWATER HEATER

As discussed in part I, the purpose of the feedwater heaters is to improve the Carnot efficiency factor for the cycle. The geometrical configuration of the feedwater heater, shown in fig. 6.a, is identical to that described in part I.

The feedwater enters the drain cooler part of the heater and proceeds to the condensing part. The drain cooler acts as a counterflow heat exchanger and the condensing part as a heat exchanger with a steam phase on the shell side.

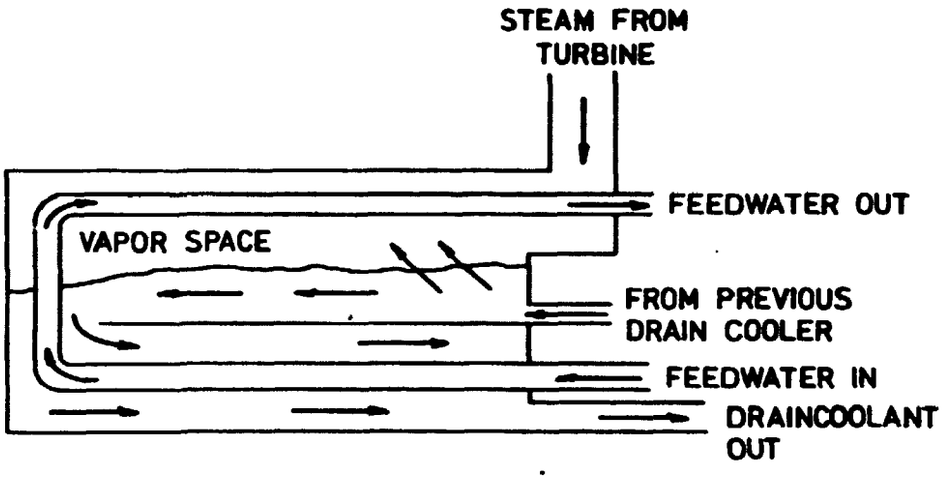

Fig. 6.a. Sketch of a feedwater heater with drain cooler.

Analogous with the model of the reheater, a lumped parameter model is used to describe the dynamics of the feedwater heater. The drain cooler part is divided into two sections with equal volumes and the same is the case for the condensing part. These four sections are shown in fig. 6.b.

The feedwater enters the first section of the drain cooler DC1 with the temperature $T_{FW,i}$. Here it is heated to the temperature $T_{FWD,a}$ and proceeds to section DC2 where it is heated to the temperature $T_{FW,o}$. Then the feedwater enters the first section of the condensing part C1, being heated to the temperature $T_{FWC,a}$ before it finally enters section C2, where it is heated to the outlet temperature $T_{FWC,o}$.

The extraction steam coming from the turbine $\dot{m}_{EX}$ is assumed to be distributed equally in the two sections C1 and C2 and, giving up its heat of evaporation by condensation on the feedwater tubes, it drops to the bottom of sections C1 and C2. The temperature of this condensate is T_{FWp}, where T_{FWp} is the saturation temperature corresponding to the pressure p_{FW} in the two sections. If the extraction steam is wet and thus enters the feedwater heater with the steam quality x_{EX}, only the part $\dot{m}_{EX}\, x_{EX}$ condenses on the tubes; the liquid part $\dot{m}_{EX}(1-x_{EX})$ drops directly to the bottom.

Drains from previous feedwater heaters, and perhaps from moisture separator and reheater, enter the condensing section C1, where some of them may flash and thus be mixed with the steam coming from the turbine; the liquid part that remains drops to the bottom of the condensation rooms.

The total mass M_L of the condensate standing on the bottom of these two sections, together with the temperature T_L, is calculated at each time step.

Leaving the bottom of section C1 with the temperature T_L, the condensate enters section DC2, where it is heated to the temperature $T_{DC,a}$. Finally, the drain enters section DC1, being heated to the outlet temperature $T_{DC,o}$.

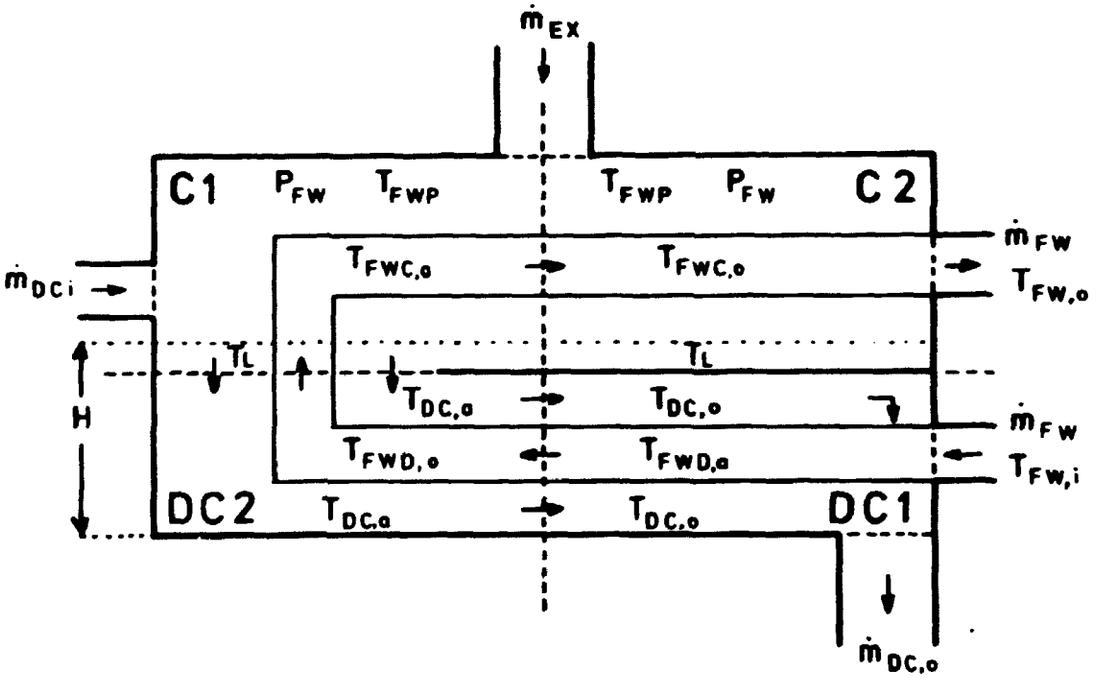

Fig. 6.b. Division of the feedwater model into the four sections C1, C2, DC1 and DC2 shown by the dashed lines.

In order not to overflow sections C1 and C2, the water level H must be kept within certain limits. This is achieved by a level regulation valve located on the drain line to the next feedwater heater downstream; a description of this regulation valve will be given later.

6.1. The Energy Balance Equations for the Four Heater Sections

The energy balance equations for section DC1 can be written as

$$\frac{dT_{FWD,a}}{dt} = \frac{\dot{m}_{FW}}{M_{FWDC1}}(T_{FW,i}-T_{FWD,a}) + \frac{(UA)_{DC}}{C_p \cdot M_{FWDC1}}(T_{DC,o}-T_{FWD,a})$$

$$\frac{dT_{DC,o}}{dt} = \frac{\dot{m}_{DC,o}}{M_{DC1}}(T_{DC,a}-T_{DC,o}) - \frac{(UA)_{DC}}{C_p \cdot M_{DC1}}(T_{DC,o}-T_{FWD,a})$$

$$M_{FWDC1} = V_{FWP1} \cdot \rho_f ; \qquad M_{DC1} = V_{DCP1} \cdot \rho_f$$

where V_{FWP1} is the volume of the feedwater pipes situated inside section DC1, and V_{DCP1} is the volume of the drain cooler pipes situated inside section DC1. ρ_f is the density of water and C_p is the specific heat of water at constant pressure.

Similarly the equations for section DC2 can be written as

$$\frac{dT_{FWD,o}}{dt} = \frac{\dot{m}_{FW}}{M_{FWDC2}}(T_{FWD,a}-T_{FWD,o}) + \frac{(UA)_{DC}}{C_p \cdot M_{FWDC2}}(T_{DC,a}-T_{FWD,o})$$

$$\frac{dT_{DC,a}}{dt} = \frac{\dot{m}_{DC,o}}{M_{DC2}}(T_L-T_{DC,a}) - \frac{(UA)_{DC}}{C_p \cdot M_{DC2}}(T_{DC,a}-T_{FWD,o})$$

where it is assumed that the heat transfer coefficient times the area $(U \cdot A)_{DC}$ is equal for the two sections DC1 and DC2. Further, it is assumed that $M_{FWDC2} = M_{FWDC1}$ and $M_{DC2} = M_{DC1}$.

The energy equation for section C1 becomes

$$\frac{dT_{FWC,a}}{dt} = \frac{\dot{m}_{FW}}{M_{FWC1}}(T_{FWD,o}-T_{FWC,a}) + \frac{(UA)_C}{C_p \cdot M_{FWC1}}(T_{FWp}-T_{FWC,a})$$

and for section C1

$$\frac{dT_{FWC,o}}{dt} = \frac{\dot{m}_{FW}}{M_{FWC2}}(T_{FWC,a}-T_{FWC,o}) + \frac{(UA)_C}{C_p \cdot M_{FWC2}}(T_{FWp}-T_{FWC,o})$$

where again it is assumed that $(UA)_C$ has the same value for the two sections C1 and C2. Further, $M_{FWC2} = M_{FWC1} = V_{FWC1} \cdot \rho_f$ with V_{FWC1}

expressing the volume of the part of the feedwater pipe situated inside section C1.

6.2. Determination of the Pressure on the Shell Side of the Heater

A mass balance equation for the steam phase in the two condensing sections C1 and C2 can be written as

$$\frac{dM_{FWg}}{dt} = x_{EX} \cdot \dot{m}_{EX} + \dot{m}_{DCg} - \dot{m}_C$$

where M_{FWg} is the total steam content in the two sections, $\dot{m}_{DCg}$ is the part of the drain coming from the previous heater that flashes in section C1, and $\dot{m}_C$ is the mass flow rate of steam condensing on the feedwater tubes.

The mass flow rate of extraction steam is calculated from

$$\dot{m}_{EX} = A_{EX}\left[\frac{n}{n-1}\left(\frac{p_{EX}}{v_{EX}}\right)\left(\left(\frac{p_{FW}}{p_{EX}}\right)^{2/n} - \left(\frac{p_{FW}}{p_{EX}}\right)^{\frac{n+1}{n}}\right)\right]^{1/2}$$

where the area A_{EX} is determined from the steady-state calculation with "TURBPLANT" and assumed constant during the dynamic calculation.

The flashing term $\dot{m}_{DCg}$ is calculated from

$$\dot{m}_{DCg} = \frac{\dot{m}_{DC,i}(h_{DC,i} - h_f)}{h_g - h_f}$$

where $h_{DC,i}$ is the specific enthalpy of the drain coming from the previous heater, and h_f and h_g are the specific enthalpies of water and steam evaluated at the saturation pressure p_{FW}.

Finally $\dot{m}_C$ is calculated from

$$\dot{m}_C = \frac{(UA)_C}{(h_g - h_f)}(T_{FWp} - T_{FWC,a}) + \frac{(UA)_C}{(h_g - h_f)}(T_{FWp} - T_{FWC,o}) .$$

Thus, being able to calculate the total steam mass M_{FWg} at each time step, it is possible to determine the pressure as time proceeds by assuming saturated conditions for the steam phase in the two sections. This is carried out by means of the function

$$p_{FW} = PSAT(v_{FW})$$

with

$$v_{FW} = \frac{V_{C1} + V_{C2}}{M_{FWg}} .$$

The mass M_L and the temperature T_L of the condensate standing in the bottom of the condensing room can finally be determined by means of the following two balance equations for mass and energy

$$\frac{dM_L}{dt} = \dot{m}_C + \dot{m}_{EX}(1-x_{EX}) + \dot{m}_{DC,i} - \dot{m}_{DCg} - \dot{m}_{DC,o}$$

$$\frac{dT_L}{dt} = \frac{1}{M_L} [(\dot{m}_C + \dot{m}_{EX}(1-x_{EX}) + \dot{m}_{DC,i} - \dot{m}_{DCg}) T_{FWp} - \dot{m}_{DC,o} \cdot T_L].$$

6.3. The Solution Method for the Differential Equations of the Feedwater Heater

From the steady-state solution with "TURBPLANT" carried out at nominal conditions, all the mass flow rates are known together with the shell side pressure and the inlet and outiet temperatures. By setting the time derivatives for the differential equations derived in section 6.1 to zero, the heat transfer coefficients $(UA)_C$ and $(UA)_{DC}$ and the temperature $T_{FWD,a}$, $T_{FWD,o}$ can be calculated. During the succeeding dynamic calculation the heat transfer coefficients $(UA)_C$ and $(UA)_{DC}$ are assumed to be constant.

The nine coupled differential equations derived in sections 6.1 and 6.2 describing the dynamics of a feedwater heater are then solved by the matrix exponential method. Because of the large volume of the feedwater heater, the temperatures vary rather slowly even during large transients and the time step used in the integration method can thus be up to 50 milliseconds.

Finally it must be mentioned that the equations derived here for a single feedwater heater are set up for every feedwater heater in the cascade; the model can handle up to ten feedwater heaters in a cascade.

7. THE FEEDWATER PUMP

The dynamics of the feedwater pump was not studied in detail, mostly due to lack of time, but also because this feature is of more interest from a regulation point of view in this plant model.

The purpose of the feedwater control system is to regulate the feedwater flow, so that the water level in the reactor vessel is maintained according to the requirements of the steam separators, and to prevent uncovery of the reactor core during load changes. This is achieved by measuring both the steam load $\dot{m}_{sl}$ and the water level H_W and by regulating the feedwater flow $\dot{m}_{FW}$ according to these measurements.

In the model it is assumed that this regulation can be described by the following second-order differential equation

$$\tau_1 \cdot \tau_2 \frac{d^2 \dot{m}_{FW}}{dt^2} + (\tau_1 + \tau_2) \frac{d \dot{m}_{FW}}{dt} + \dot{m}_{FW} = \dot{m}_{sl} + (H_{Wo} - H_W) \cdot C_1$$

where τ_1 and τ_2 are two time constants normally of the order of a few seconds, H_{Wo} the optimum water level, H_W the actual water level, and C_1 a constant.

8. CONTROL SYSTEMS

In this section some control systems are presented for the different parts of the power plant. Some of the systems described are based on information from GESSAR, the General Electric Standard Safety Analysis Report, ref. 7. Only the main control systems are considered in the model, and they are treated in a rather simplified way.

Because of lack of information on the numerical values of numerous parameters in the control systems taken from GESSAR, control systems for pressure and for the recirculation pumps were designed, using the same control principles as outlined in GESSAR. A classical frequency analysis was used to determine the values of the control parameters; this analysis is described in appendix B.

8.1. The Water Level Control System

At the outlet of the earlier-mentioned drainage tanks for moisture separator and reheater, level regulation valves are located to avoid overflow of these tanks during fast transients. Fig. 8.1.a shows how this level

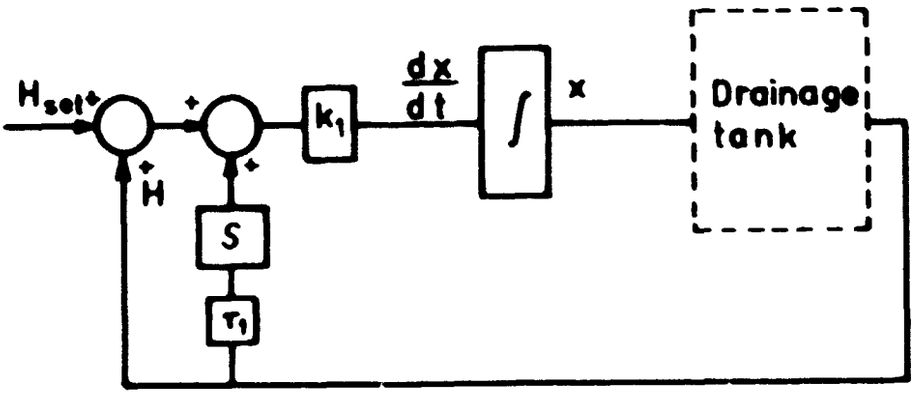

Fig. 8.1.a. Diagram of the water level control system.

regulation system is simulated in the model. H_{set} is the water level that must be maintained by the control system, the integration box simulates the movement of the valve, k_1 is an amplification factor, and S, τ_1 represents a differentiating term.

It is assumed that the actual water level H is measured without any particular time lag. The difference between the actual level and the level required is then used to move the valve. The differential equation for the control system can be written as

$$\frac{dx}{dt} = k_1(H - H_{set} + \tau_1 \frac{dH}{dt})$$

where x represents the valve position, with x = 0 corresponding to a closed valve and x = 1.0 to a completely open valve.

The mass flow rate through the valve $\dot{m}_{Valv}$ is calculated from the equation for water flow through a valve presented in 4.2,

$$\dot{m}_{Valv} = k \frac{A}{\sqrt{1-A^2}} \sqrt{\frac{2(p_1 - p_2)}{v_1}}$$

where index 1 refers to the conditions upstream of the valve and index 2 to the conditions downstream. The parameter k is assumed to be equal to 1.0, and the area A is then determined from a nominal steady-state calculation with "TURBPLANT". The area thus determined, A_o, is assumed to correspond to the valve being half open. The relation between the valve position x and the actual area A then becomes

$$A = 2 \cdot A_o \cdot x, \qquad x(o) = 0.5$$

As outlined in section 4.2 for the reheater drainage tank, the total weight of the water and its temperature are calculated at each time step. The water levels H_{set} and H are therefore replaced in the control diagram by the total weights M_{set} and M.

With M_{set}, τ_1 and k_1 given as input parameters, the valve position x is thus calculated at each time step using the Euler method.

Finally it must be mentioned that a similar water level control system is used for the condensation rooms in every feedwater heater with the regulation valve located at the drain line to the next heater and for the moisture separator drainage tank.

8.2. Regulation of the Reheating Temperature

In order to keep the reheating temperature constant under different load conditions, the inlet mass flow rate to the primary side is controlled by a valve located on the line between the reactor and the reheater.

It is assumed that the outlet temperature on the secondary side of the reheater $T_{RH,o}$ is measured without any time lag. The difference between the temperature required and the measured temperature is then used to regulate the valve position in a way similar to that in fig. 8.1.a.

The mass flow rate through the valve $\dot{m}_{RHP}$ is calculated by the expression (4.2.4.a) derived in section 4.2, and with T_{set}, τ_1 and k_1 known the valve position can be calculated at each time step from

$$\frac{dx}{dt} = k_1 (T_{set} - T_{RH,o} - \tau_1 \frac{dT_{RH,o}}{dt}), \qquad x(o) = 0.5$$

and the valve area from

$$A = 2 \cdot A_o \cdot x$$

where A_o is known from the steady-state calculation.

8.3. Regulation of the Reactor System Pressure

In fig. 8.3.a is shown a principle diagram of the pressure control and recirculation flow control system used in the model. If the plant is running at load-following conditions, the pressure control and recirculation systems work together. The pressure is regulated by adjusting the turbine regulation valve and the recirculation flow by adjusting a valve in the reactor

circulation pump system located in the downcomer. If e.g. a load/speed error from the turbine governor, corresponding to a demand of increased power level, is measured, a signal is transmitted to the pressure regulator and to the circulation pumps. The pressure control signal lowers the setpoint value of the pressure regulator and thus causes a fast opening of the turbine regulation valve to meet the increase in power demanded. The recirculation flow signal causes an increase in the flow through the core by an increased opening of the pump valve. This leads to a decrease in the void content in the core and thus to an increased neutron flux. When the recirculation flow change affects the increase in reactor power level, the setpoint value of the pressure regulator slowly returns to its original value. When a power decrease is demanded, the pressure setpoint is increased and the pump valve area decreased and a flow pattern with a higher void content in the core is established; in the case of a very fast power decrease the bypass valve may open also. During the regulation procedure the reactor system pressure must be kept within certain limits in order not to cause reactor scram, normally 4 bar is allowed on both sides of the system pressure.

During the above-mentioned regulation it has been assumed that the control rod pattern is kept constant. This is partly because the model is based on the point kinetics equation, and thus unable to handle control rod motions, and partly because in reality the recirculation flow control system alone is used to change the power level during normal operation. At a certain power level and control rod pattern, the power can thus be increased by about 25% just by increasing the flow rate of the recirculating water in the reactor.

If the plant is running at base-load conditions the setpoint value of the pressure regulator is kept constant and the pressure control system operates independently of the flow control system and the load/speed error signal. The steam flow to the turbine is thus determined by the requirement of constant pressure in the reactor.

The turbine valve is regulated by throttling, i.e. a process where the enthalpy is constant across the valve. The mass flow rate through the valve is again given by

$$\dot{m} = A\left[\frac{n}{n-1}\left(\frac{p_R}{v_R}\right)\left(\left(\frac{p_T}{p_R}\right)^{2/n} - \left(\frac{p_T}{p_R}\right)^{\frac{n+1}{n}}\right)\right]^{1/2}$$

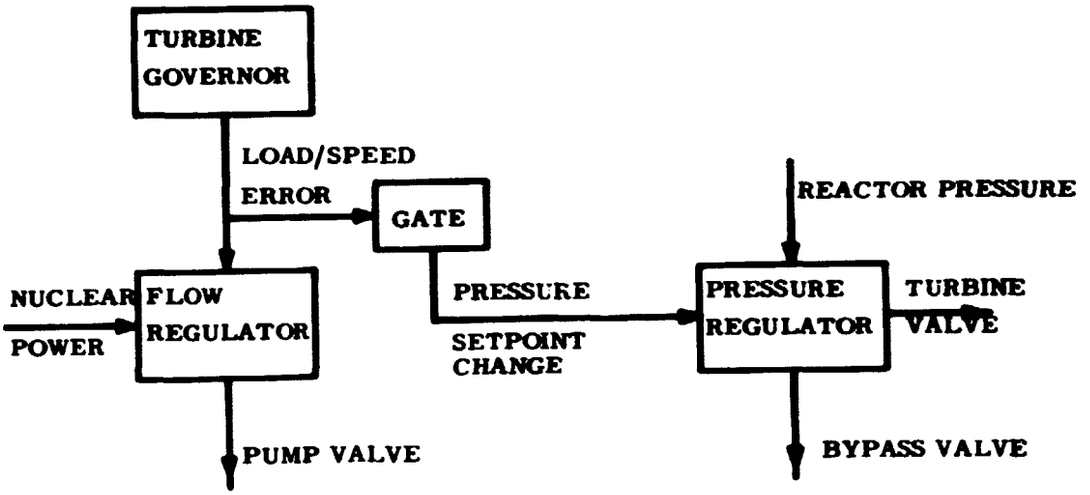

Fig. 8.3.a. Flow chart of the pressure control and recirculation flow control system.

with A as the valve area, p_R the reactor pressure, and p_T the pressure in a room located at the inlet of the high-pressure turbine. In order to find the pressure p_T at each time step, this room is treated in the same way as the extraction rooms for feedwater heaters, apart from the fact that only the mass balance equation is necessary because the specific enthalpy of the mixture in the room is constant.

In fig. 8.3.b is shown the diagram for the pressure control system used in the model. A load/speed error signal is received from the turbine governor and sent through a gate with three different output values. In the existing version of the model the required grid power, as function of time, must be given as input parameter. The load/speed error is then simulated as the difference between the required grid power and the power generated by the turbine. If the numerical value of the error signal is very low, the output of the gate will be 70 bar; if the error signal is positive the output will be 73 bar, and if it is negative, the output will be 67 bar. The difference between the actual reactor pressure p_R and the setpoint value p_{set} is then added to a signal representing the derivative of the pressure, and we thus have a PD-regulator, or a proportional and differentiating regulator. This signal is then applied to move the turbine valve, which again affects the reactor pressure. If the pressure exceeds 74 bar, the bypass valve is actuated through a low value gate.

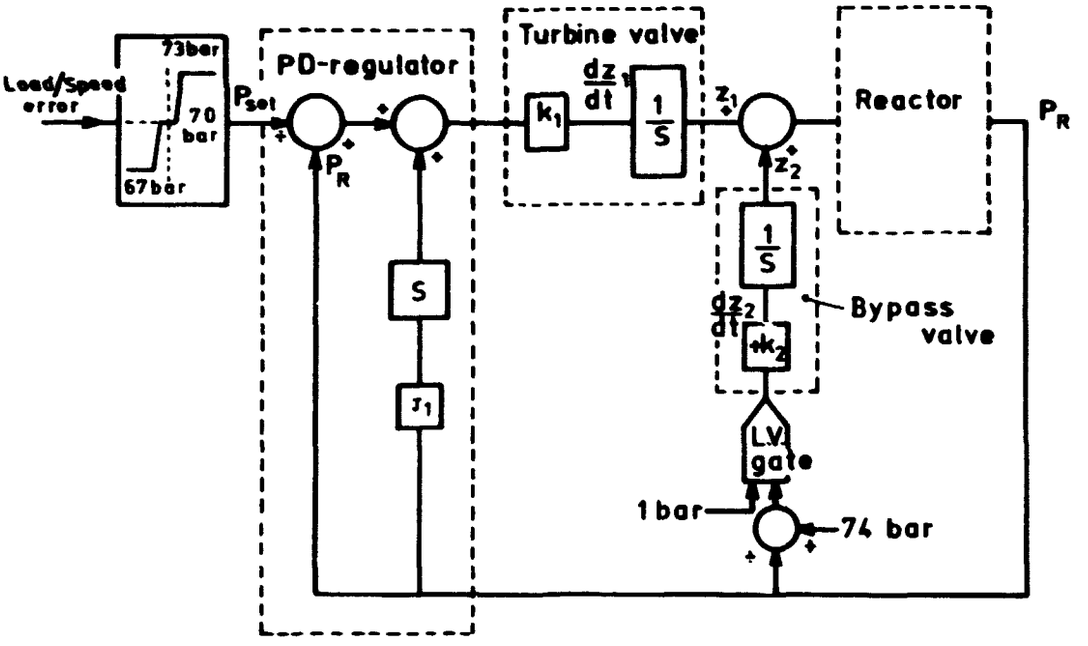

Fig. 8.3.b. Diagram of the pressure control system using a PD-regulator.

The values of the amplification parameters k_1 and k_2 and the time constant τ_1 depend on the power plant considered; they are thus input parameters for the model. For a given plant, they can be determined from a frequency analysis.

The differential equations for the pressure control system become

$$\frac{dz_1}{dt} = k_1\left(p_R - p_{set} + \tau_1 \cdot \frac{dp_R}{dt}\right) \qquad z_1(o) = 0.5$$

$$\frac{dz_2}{dt} = -k_2(74 \text{ bar} - p_R) \qquad z_2 < o \Rightarrow z_2 = o$$

$$z_2(o) = o$$

where z_1 is the position of the turbine valve with $A_T = 2 \cdot z_1 \cdot A_{To}$ and z_2 is the position of the bypass valve with $A_B = 2 \cdot z_2 \cdot A_{Byo}$; A_{To} and A_{Byo} are calculated from the steady-state solution.

Euler's method is used to calculate z_1 and z_2 at each time step.

8.4. The Recirculation Flow Control System

In fig. 8.4.a is shown a diagram for the recirculation flow control system. The load/speed error signal is here again replaced by the required grid power and, in order to compare it with the nuclear power, the grid power is further multiplied by a factor 3. Regulation is then carried out by means of a PID-regulator or proportional, intergrating and differentiating regulator. This regulator affects a pump valve, in the model simulated as a pump head decrease or increase, which then causes a corresponding change of the nuclear power N.

The differential equations for the control system become

$$\frac{dz_1}{dt} = (N_{set} - N)$$

$$\frac{dz_2}{dt} = (z_1 + \sigma_1(N_{set} - N) - \tau_1 \frac{dN}{dt}) \cdot k_2$$

where z_2 is the pump head.

These two equations are solved at each time step by Euler's method.

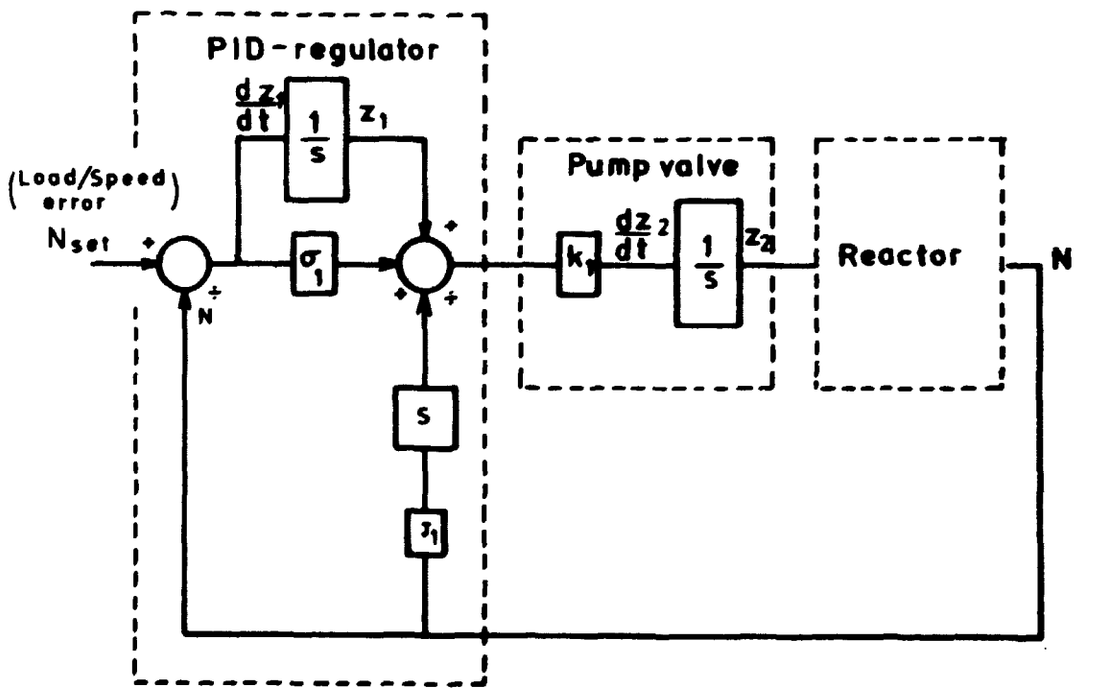

Fig. 8.4.a. Diagram of the recirculation flow control system using a PID-regulator.

In appendix B is given an example of determination of the parameters of the above-mentioned flow control system by means of classical frequency analysis.

9. OVERALL PLANT CALCULATION

All the different sub-models contained in the overall dynamic plant model, named "BWRPLANT", have now been described, and in fig. 9.a is shown a flow diagram of the total plant model with six feedwater heaters as example. The dashed lines represent the control systems.

Fig. 9.b shows the corresponding flow chart for the calculation procedure of "BWRPLANT". The grid power, as function of time, is the perturbating quantity given as input to the model. The difference between the grid power and the power produced is led partly to the recirculation flow control system and partly to the pressure control system. The recirculation system affects the nuclear power of the reactor, and the reactor dynamics is calculated as earlier shown in fig. 2.4.a. The pressure control system attempts to keep the reactor pressure constant, but with the grid/turbine error signal or load/speed error signal overriding the pressure setpoint value, provided that it is within the reactor scram limits. The calculation then continues with the high-pressure turbine and, via the moisture separator-reheater calculation with drain tank level control, it proceeds to the low-pressure turbine; the turbine power to be compared with the grid power at the next time step is now determined. After the calculation of the hold-up tank in the condenser, the feedwater cascade calculation with water level control starts, and via the feedwater regulation system, the inlet conditions to the reactor to be used in the next time step are finally determined. Then the procedure starts all over again, with the grid power to the next time step as a new perturbating quantity.

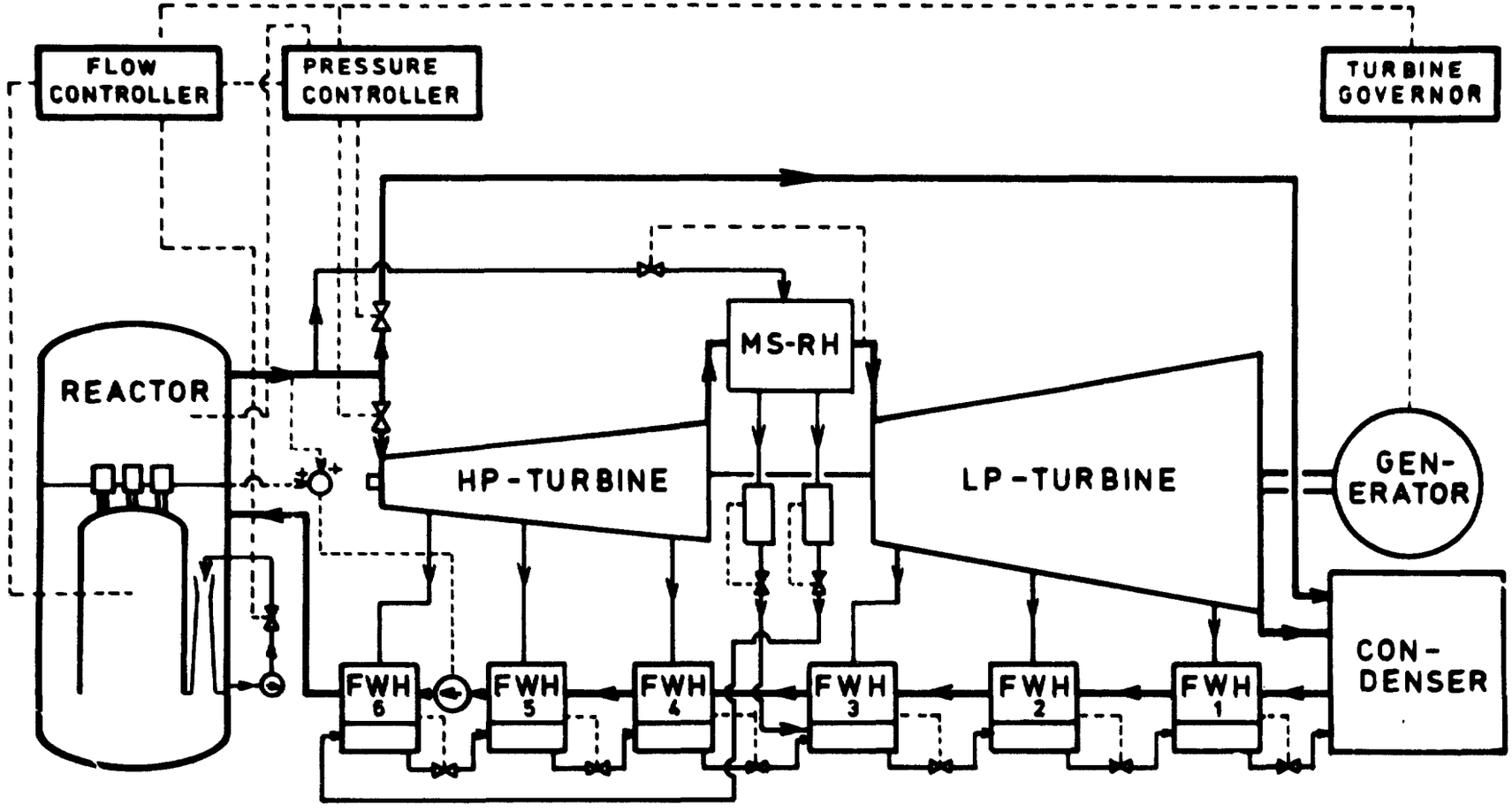

Fig. 9.a. Flow diagram of the total plant model with 6 feedwater heaters as example. The dashed lines represent the control systems.

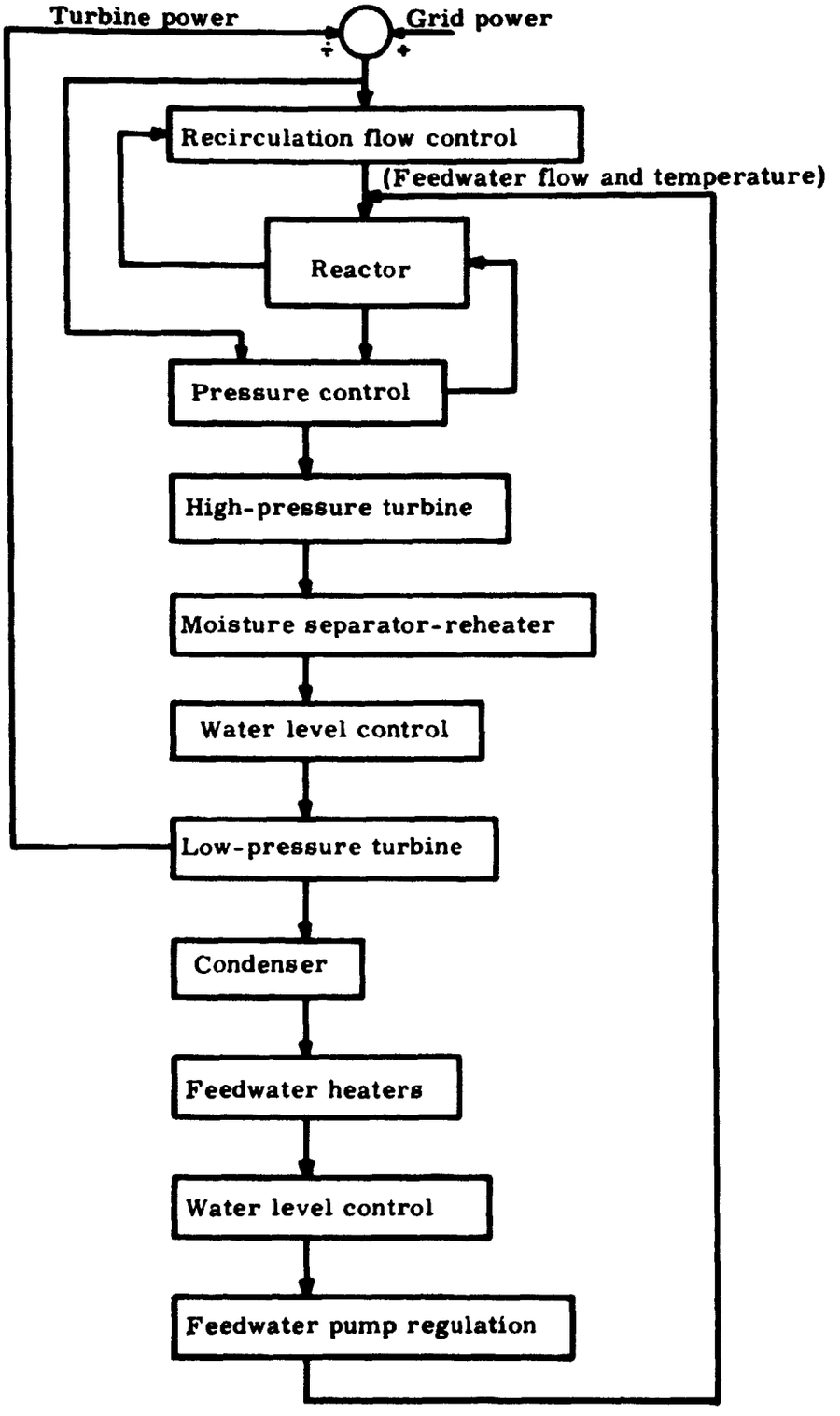

Fig. 9.b. Flow chart for the calculation procedure of "BWRPLANT".

9.1. Integration Methods

Three different integration methods are used

1) Matrix exponential method

2) Modified Euler

3) Simple Euler

The matrix exponential method is used for the reheater integration and feedwater heater integration with constant time step of either 20 or 50 ms. The modified Euler method is used for calculation of the turbines with time steps from 5 to 10 ms. The simple Euler method is used for integration of the remainder of the plant, that means firstly the reactor and then the control systems.

Equal time steps are used for the two Euler methods. The time step is selected partly on the basis of the relative error demands and partly on the basis of the numerical stability limits.

The integration of the turbine caused much trouble because of numerical instabilities. First the simple Euler method was applied, but due to the high flow velocities in the turbine this became unstable for time steps larger than 2 ms; further, with such small time steps the computing time for the whole plant would be inadmissibly large. Then the modified Euler method was applied, and this gave a great improvement of stability, even with time steps of the order of 5 to 10 ms. Nevertheless it is turbine integration that determines the time step to be used for the two integration methods with the stability limits as the governing quantity. The stability limits are calculated from the relation $\lambda \cdot \Delta t < 2.5$, ref. 8, where λ is the convergence radius, calculated in the model by an approximate method, and Δt is the time step. The demand for a relative error of less than 0.0001 is fulfilled with the time step calculated from the stability limits. Thus the time steps for the two Euler methods vary, while the time step for the matrix exponential method is kept constant.

The ratio between computing time and power plant time is about 35 to 1 for the Burroughs B-6700 computer, depending on the number of sections chosen in the reactor and in the turbine. One third of this computing time is spent on the reactor and two-thirds on the remainder of the plant with the turbine calculation as the most time-consuming.

Finally, it should be mentioned that the functions for thermal properties of steam and water presented in part I of this report, the steady-state model, are also implemented in the dynamic model.

10. TRANSIENT STUDIES OF SOME SUB-MODELS OF THE OVERALL MODEL AND TESTING OF THE REACTOR MODEL

This section presents some dynamic studies of the turbine alone and of a feedwater heater alone, together with a test of the reactor model against a 3-dimensional reactor model.

10.1. Dynamic Studies of the Turbine of the Obrigheim Power Plant

A series of dynamic studies made of the turbine of the Obrigheim power plant will now be described. The technical data of the turbine are shown in section 12 in part I of this report. The basis for this dynamic analysis is the steady-state calculation at 300 MWe nominal power carried out with "TURBPLANT", the results of which are shown in figs. 12.b and 12.c in part I.

A perturbation of the inlet mass flow to the high-pressure turbine was first studied. The plant was assumed to be running at nominal power when suddenly the inlet mass flow to the high-pressure turbine regulation chamber was interrupted through the expression $m_o(1 - (\frac{t}{2})^2)$, where m_o is the inlet mass flow rate at nominal conditions and t is the time. The extraction steam for feedwater heaters was not taken into account and the number of revolutions of the turbine rotor was assumed to be constant. In fig. 10.1.a are shown the responses to this perturbation, the curve with index 1 shows the perturbating mass flow rate, the curves with indexes 2 and 3 the mass flow rates at inlet and outlet of the high-pressure turbine, and finally indexes 4 and 5 the mass flow at inlet and outlet of the low-pressure turbine. From the curves it appears that only the combined moisture separator-reheater between the two turbines causes any considerable mass flow holdup, the inlet and outlet flow of the high-pressure turbine almost coincide, and the same is the case for the low-pressure turbine.

Fig. 10.1.b shows, for the same transient, the relative pressure versus time for the high-pressure turbine inlet and low-pressure turbine inlet. These curves also indicate a time lag for the flow through the combined moisture separator-reheater.

In fig. 10.1.c is shown another mass flow transient applied to the high-pressure turbine inlet and in fig. 10.1.d the corresponding production of electrical power. It is seen that the response of the electrical power almost follows the mass flow transient without any time lag. Again this transient was carried out for the turbine of the Obrigheim power plant without taking the feedwater heater extraction flow into account.

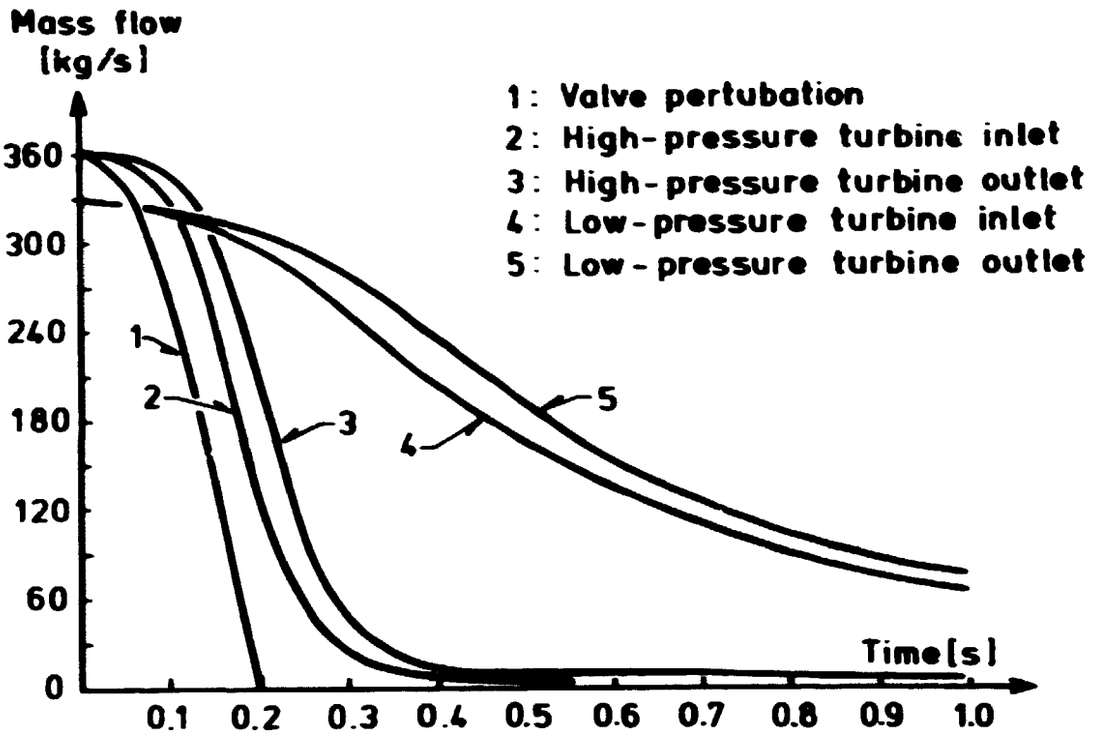

Fig. 10.1.a. Responses of the inlet and outlet flows of the Obrigheim turbine to an inlet mass flow perturbation given by $m_o (1 - (\frac{t}{2})^2)$ where m_o is the inlet mass flow rate to the high-pressure turbine at the nominal power 300 MWe.

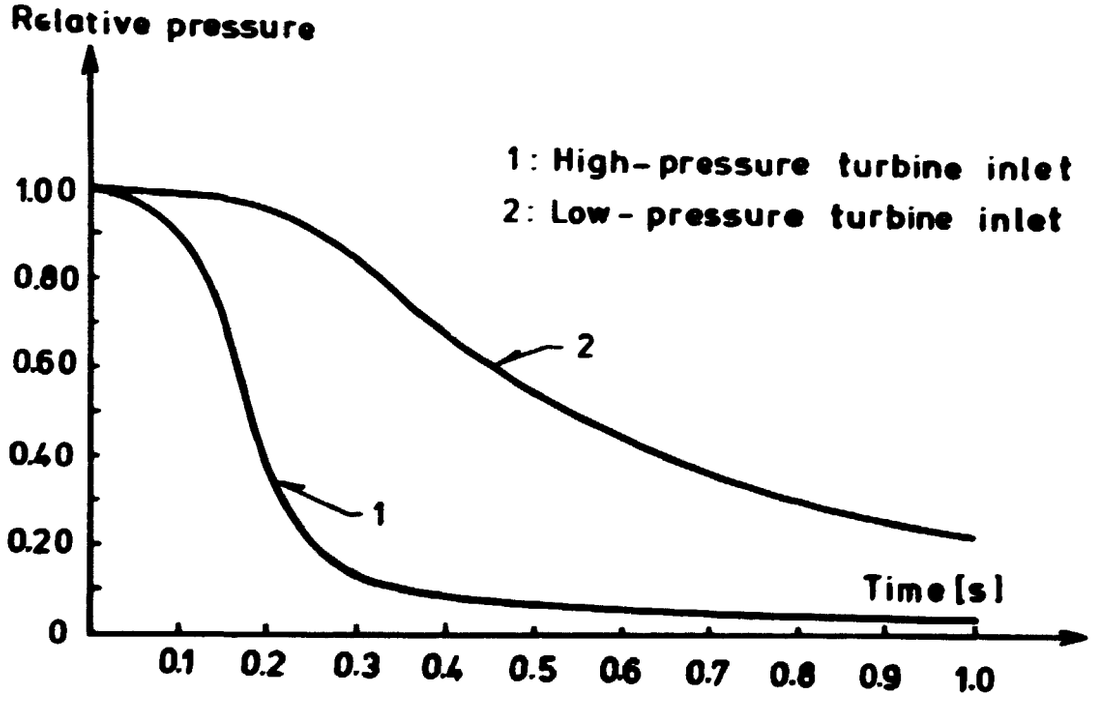

Fig. 10.1.b. Responses of the relative pressure at inlet of the high-pressure turbine and low-pressure turbine to the same perturbation.

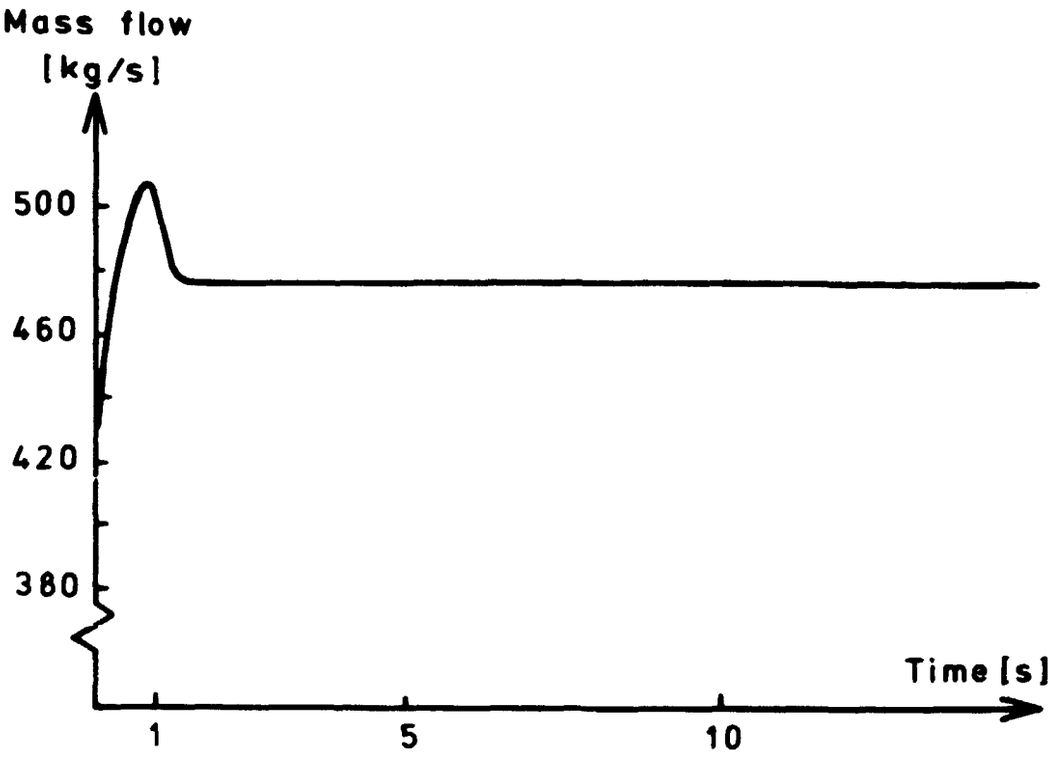

Fig. 10.1.c. A mass flow perturbation applied to the high-pressure turbine inlet.

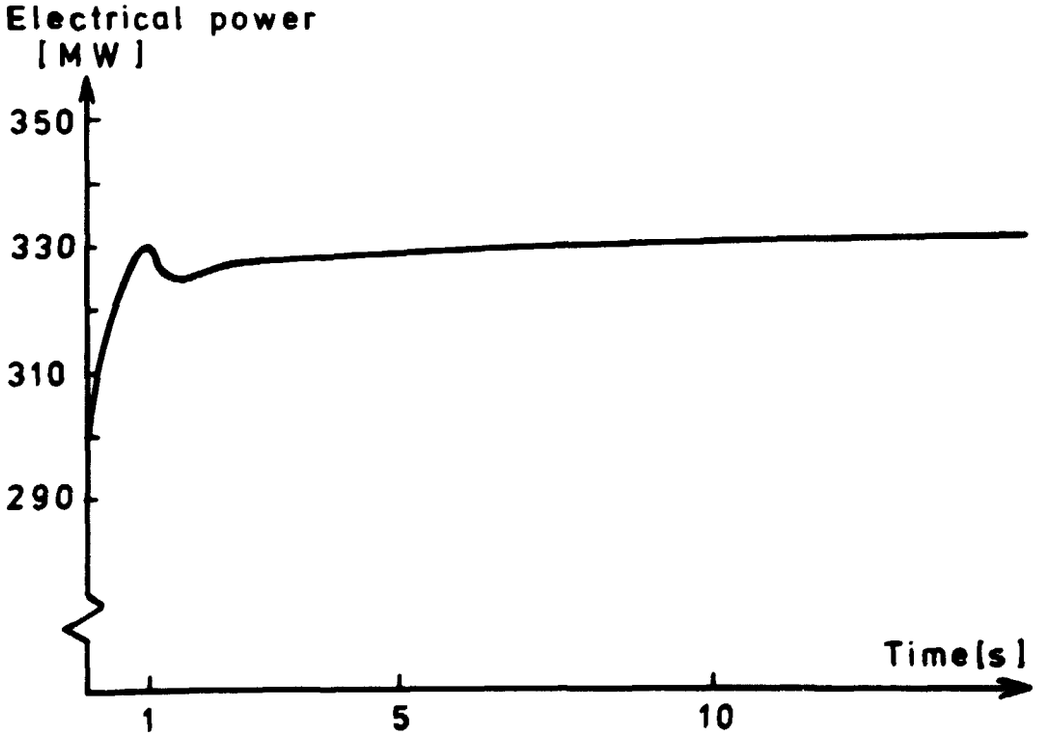

Fig. 10.1.d. The corresponding response of the electrical power production to this mass flow perturbation.

In order to study the dynamics of a single feedwater heater, a calculation was carried out where the steam flow from the turbine to the heater was decreased linearly form the nominal value to zero within 10 s. The feedwater heater chosen was one of the low-pressure heaters at Obrigheim and it was assumed that the mass flow rate of the feedwater and the mass flow rate of the drain out of the drain cooler part were kept constant at the nominal values during the transient. In fig. 10.1.e is shown the outlet temperature of the feedwater as function of time; it is seen that the temperature decreases rather fast.

A similar transient was calculated with the feedwater heater model divided into six sections instead of, as described in section 6, four sections. The results obtained were found to be almost the same in both cases.

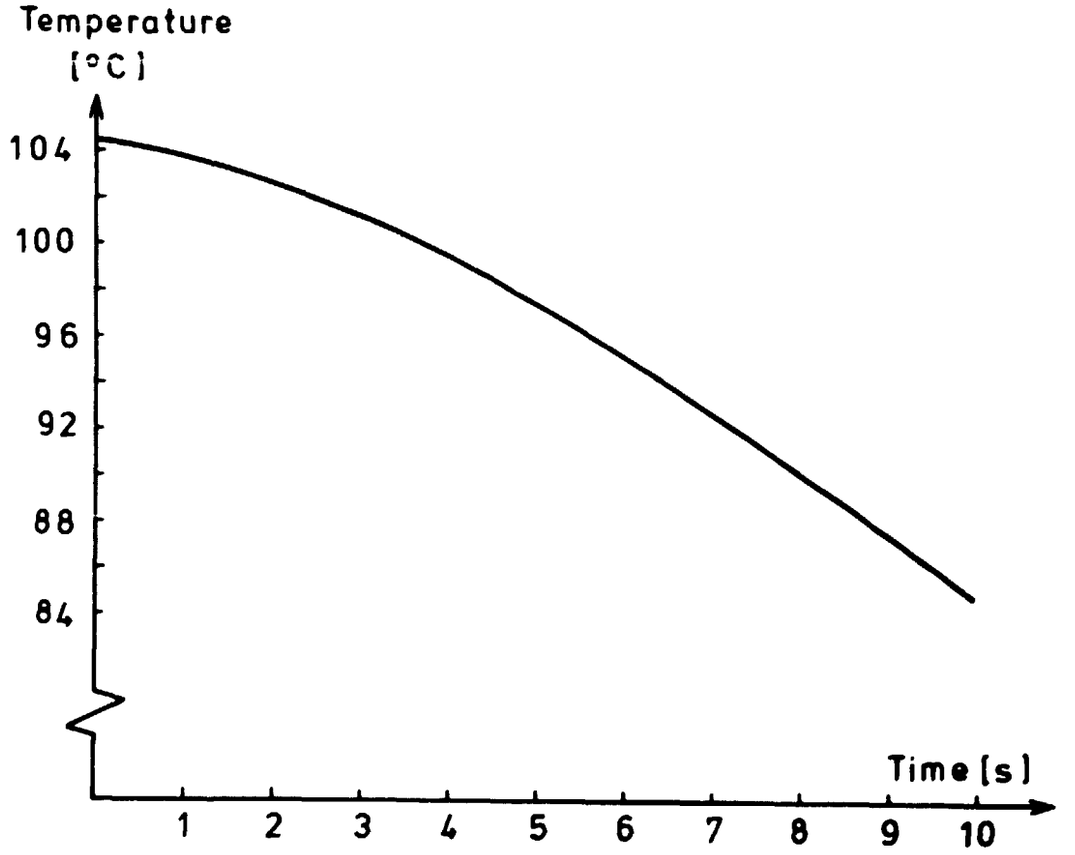

Fig. 10.1.e. The response of the outlet temperature of a low-pressure feedwater heater at Obrigheim to a linear interruption of the extraction steam flow from the nominal value to zero within 10 s.

Finally, again with the Obrigheim data, a transient was made where the extraction steam flow to the feedwater heaters was taken into account. The plant was assumed to be running at 300 MWe when suddenly the power was decreased to 225 MWe within 2.5 s. Here, as with the ealier transients described, the reactor calculation was omitted and the steam was assumed

throttled through the regulation valve with constant pressure of 50 bar upstream the valve and a varying pressure downstream corresponding to the required load on the turbine.

The decrease in steam flow to the turbine necessary to meet this fast load reduction is shown in fig. 10.1.f. The extraction steam flow versus time is shown in figs. 10.1.h and 10.1.i with the numbers referring to the feedwater heaters shown in fig. 10.1.g.

The reduction in steam flow causes the pressure in the extraction rooms to decrease, and thus the steam flow to the feedwater heaters is reduced too. In all the six curves there appears an underflow caused by the faster pressure decrease in the extraction rooms compared to the pressure decrease on the shell side of the heaters. Further, it is seen that the underflow for the three high-pressure heaters in fig. 10.1.i is far greater than the underflow for the three low-pressure heaters in fig. 10.1.h. This is due to the faster pressure decrease in the high-pressure extraction rooms than in the low-pressure extraction rooms.

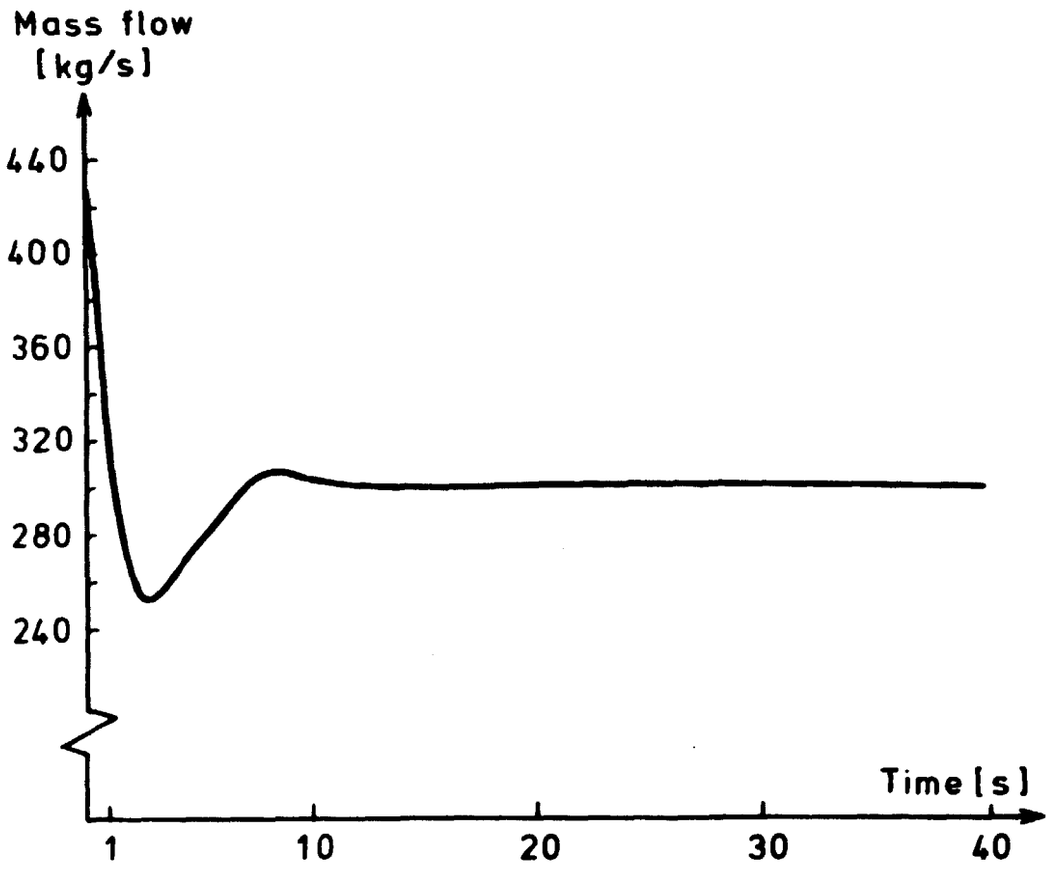

Fig. 10.1.f. The steam flow to the high-pressure turbine necessary to meet a demand for a power decrease from 300 MWe to 225 MWe within 2.5 s.

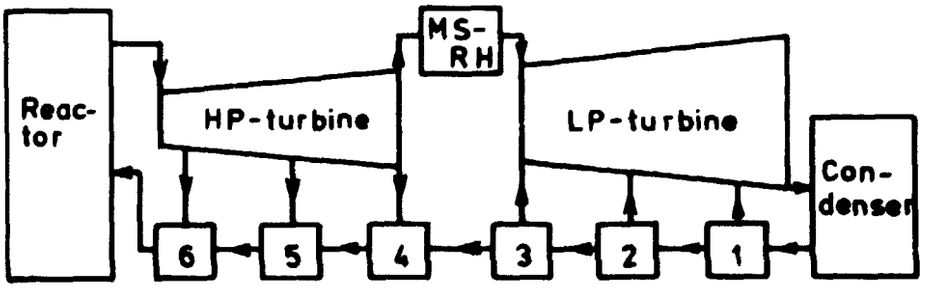

Fig. 10.1.g. Illustration of the position of the feedwater heaters.

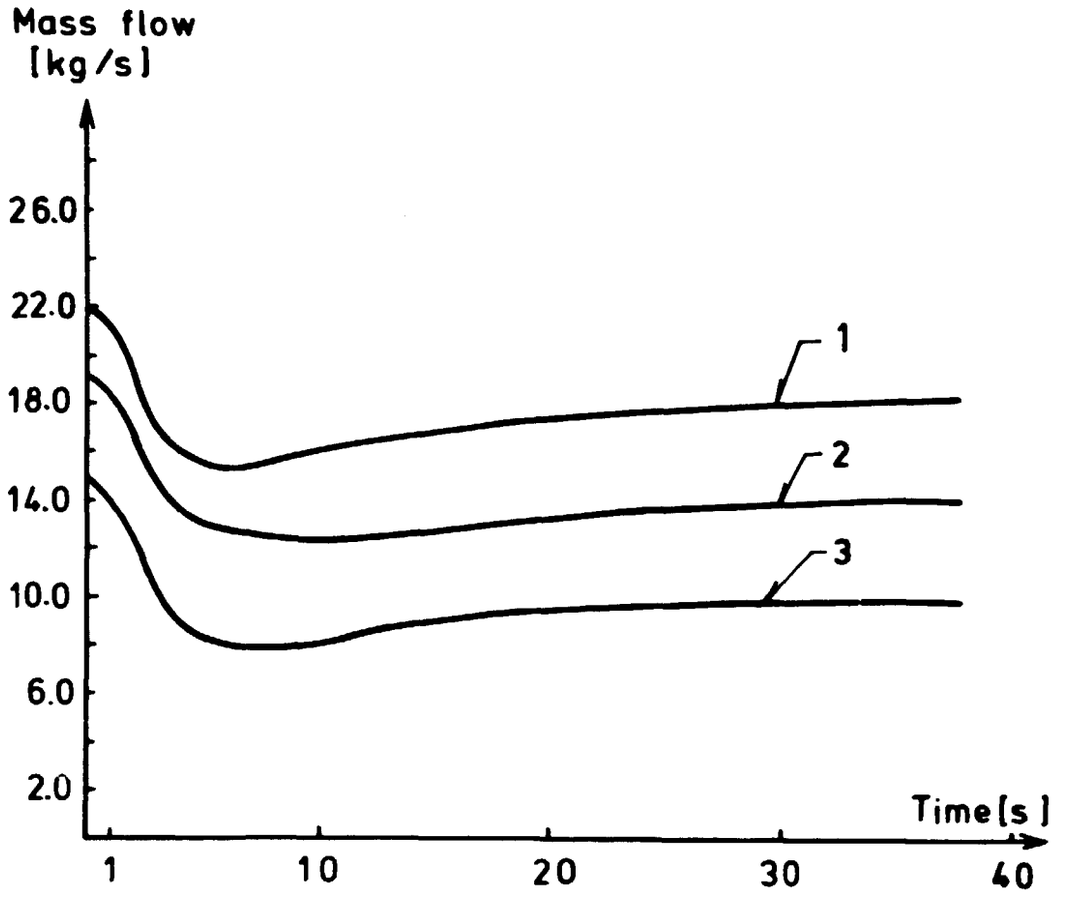

Fig. 10.1.h. The responses of the extraction steam flows leading to the low-pressure heaters.

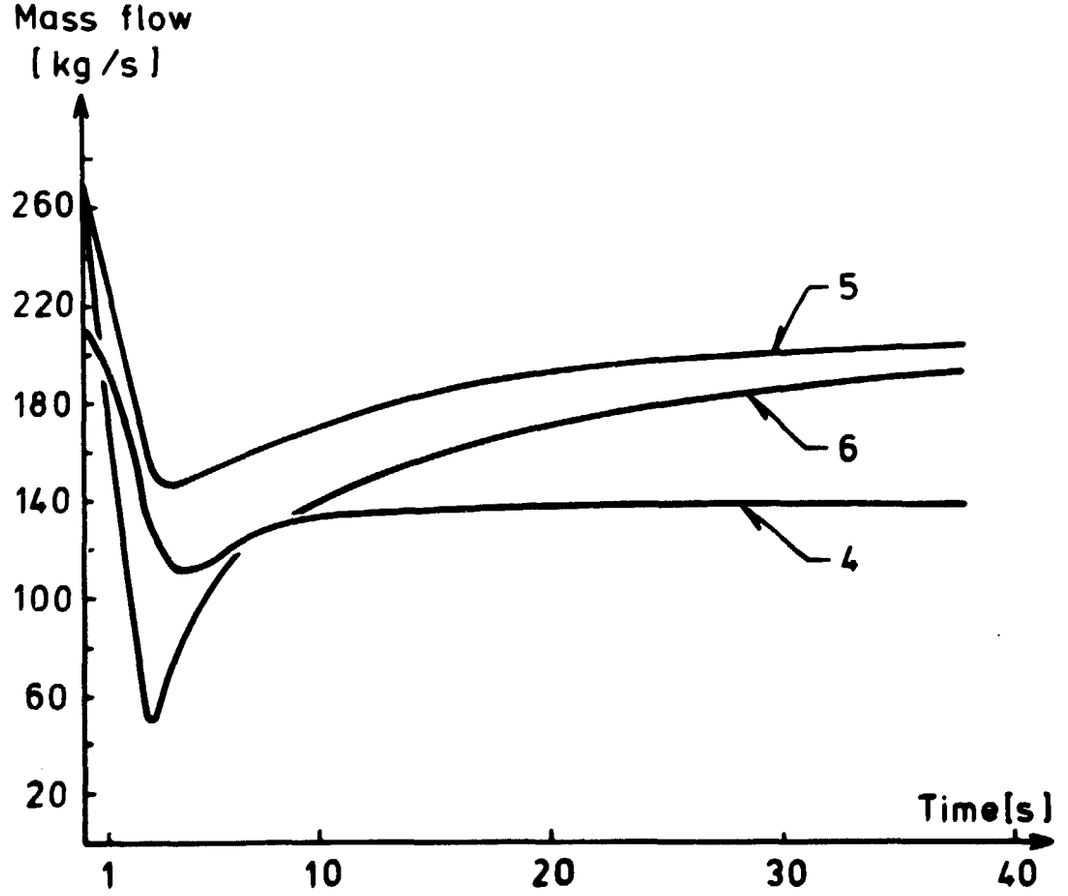

Fig. 10.1.i. The responses of the extraction steam flows leading to the high-pressure heaters.

10.2. A Comparison of the Reactor Model with a 3-Dimensional Calculation

A steam load transient made partly with "BWRPLANT" and partly with a 3-dimensional model called "ANDYCAP" is now presented. "ANDYCAP" is a very detailed, 3-dimensional model of a BWR reactor that has been tested against experiments at the Swedish BWR reactor Oskarshamn I.

As calculation example was chosen a 600 MWe BWR reactor mostly based on data from Oskarshamn II.

First a series of calculations were made with "ANDYCAP" in order to determine the void reactivity coefficient, the Doppler reactivity coefficient, and the moderator temperature reactivity coefficient to be used in the "BWRPLANT" calculation. An axial power distribution corresponding to a certain control rod pattern at 1675 MW thermal power was also calculated with "ANDYCAP" and used as input to "BWRPLANT".

At the top of fig. 10.2.a is shown the steam load perturbation applied to the two models, and below are shown the responses to this steam load perturbation expressed as the nuclear power versus time and the reactor pressure versus time.

The results obtained with the two models are seen to agree quite well in spite of the great difference between the models. This could be because the chosen steam load transient causes no local effects but only overall effects; thus the rather simple treatment of the reactor in "BWRPLANT" is sufficient.

In the above mentioned calculation the pressure control system and the recirculation flow control system of "BWRPLANT" were omitted. Finally, it should be mentioned that the calculation with "BWRPLANT" for 15 real time took about 500 s computer time; the "ANDYCAP" calculation took about 10000 s computer time.

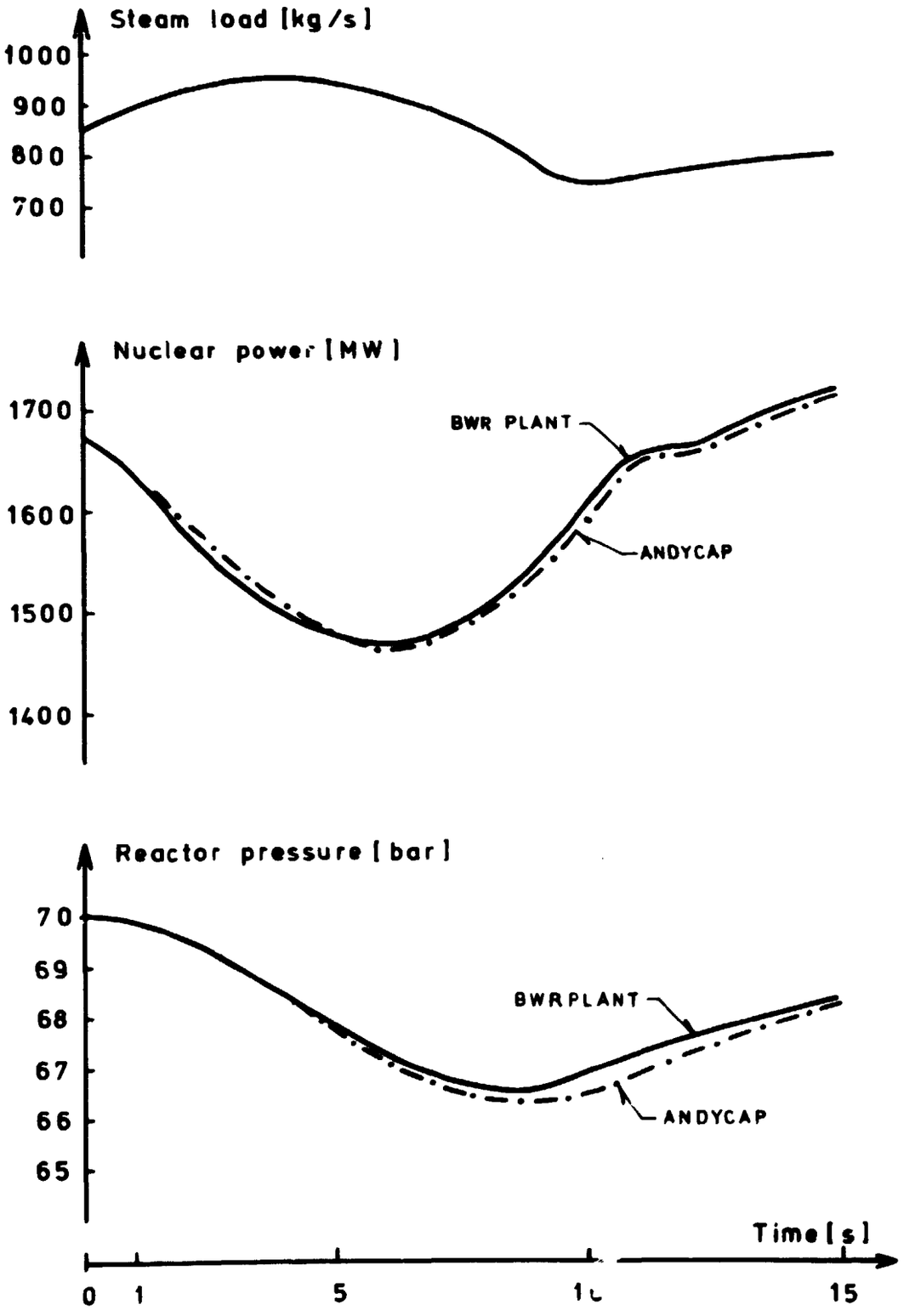

Fig. 10.2.a. Comparison between "BWRPLANT and "ANDYCAP". At the top is shown the steam load perturbation applied to the two models; below, the responses of the nuclear power and the reactor pressure.

11. PRESENTATION OF A TRANSIENT WHERE THE CONTROL SYSTEMS ARE APPLIED

A typical transient made with the model with the earlier described pressure control system and recirculation flow control system in function is now presented. The Oskarshamn II data was used for the reactor part, but, due to lack of information on the turbine data, the Obrigheim turbine data was modified in order to apply to the 600 MWe Oskarshamn plant. Also the data of reheater and feedwater heaters were taken from Obrigheim. The determination of the numerical values of the control system parameters is shown in appendix B.

It is assumed that the plant is running under load-following conditions at 560 MW electrical power when suddenly the grid demands a power increase to 616 MW electrical power within 1 s. This fast increase could, e.g., be caused by a trip of another power plant coupled to the grid.

At the top of fig. 11.a is shown the required grid power (the dashed curve) and the power produced by the turbine. It is seen that the turbine is capable of following the power demand quite well although the demanded increase is very fast. The next curves show the needed overshoot of the steam flow to the high-pressure turbine and the corresponding inlet valve position. In order to obtain this fast increase in steam flow, the reactor pressure is allowed to decrease and thus the flash effect is used to increase the steam production. The lowest curve shows the reactor pressure, and it is seen that it is well within the margin of 4 bar to avoid reactor scram. As described in the section on the pressure control system, the setpoint value of the pressure controller is determined from the load/speed error or grid power/turbine power error with the bypass valve signal overriding. The difference between the actual reactor pressure and the setpoing pressure is then used to move the turbine valve. From the curves it is seen that the valve position beyond 4 s is almost constant, though the reactor pressure is more than 1 bar below the nominal value of 70 bar. We should thus expect the valve to close slightly to return the reactor pressure to 70 bar; but this causes the load/speed error to increase and thus to open the valve, so the overall position of the valve becomes almost constant. In a large scaled system of coordinates the valve position curve oscillates slightly.

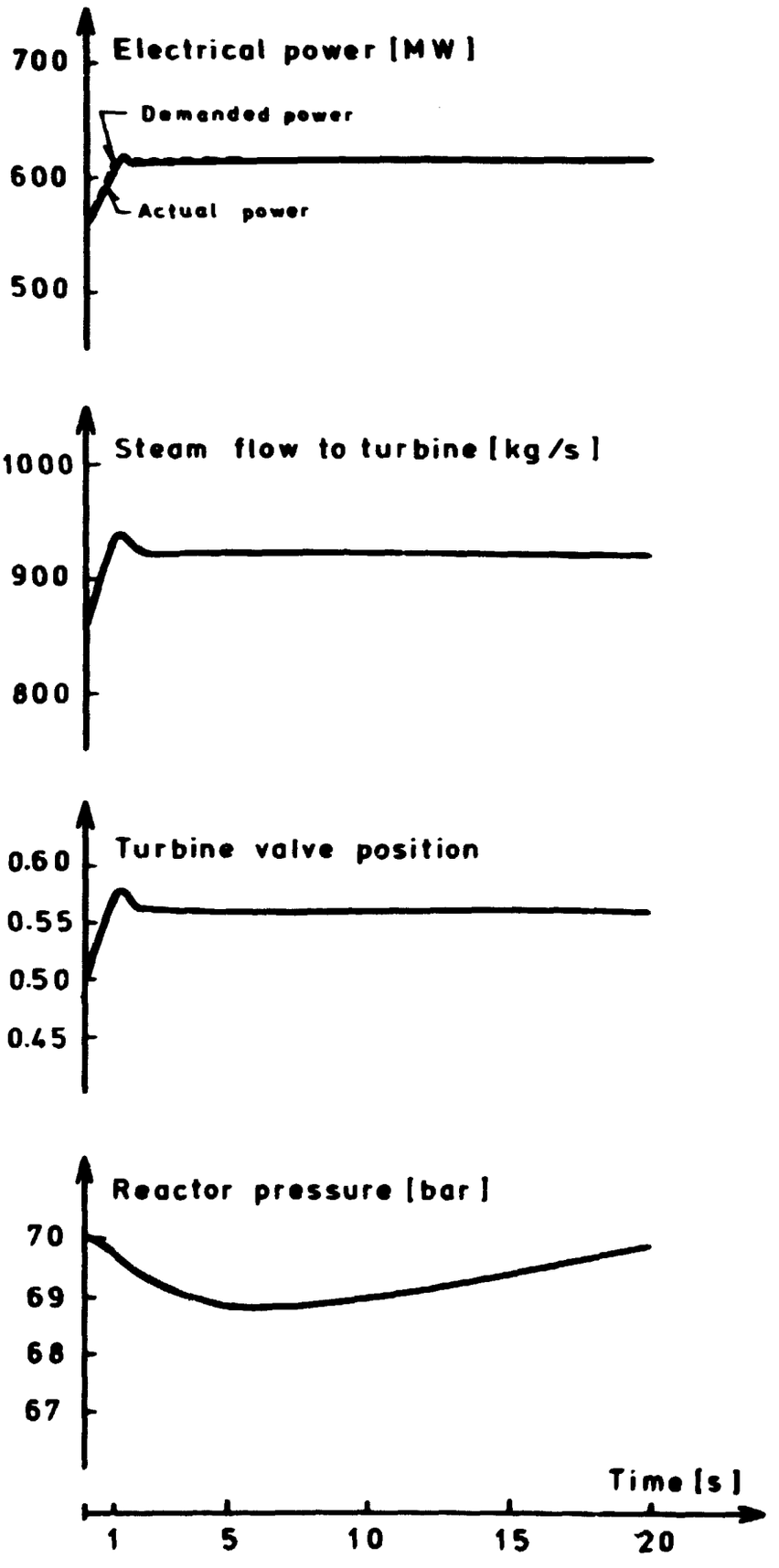

Fig. 11.a. Reeponsee to a power demand from 560 MWe to 616 MWe within 1 s.

A load/speed error signal is also transmitted to the recirculation flow control system to adjust the nuclear power. The regulation of the pump head by means of the PID-regulator, mentioned in section 8.4 is shown at the top of fig. 11.b. The next curve shows the corresponding increase in core inlet flow velocity. The average void content in the core and the nuclear power are shown in the two lowest curves. The nuclear power first decreases due to higher average void content in the core caused by the pressure decrease. After a few seconds the increased core flow velocity affects the void content in the reverse manner, and the total affect becomes a reduction in the average void content in the core. Thus the nuclear power increases and a new power level is obtained corresponding to the new flow distribution established by the increased pump head determined from the PID-regulator.

At the top of fig. 11.c is shown the thermal power delivered to the coolant. A comparison with the curve of nuclear power clearly shows how the heat capacity of the fuel causes delay of the heat flow through the fuel during transients and thus smoothes out the curve of thermal power. The next curve, showing the maximal fuel centre temperature, reflects the same characteristics. The two last curves show the water level above the riser outlet and the feedwater flow into the reactor. The rise in water level is caused by the increase in the void content. The feedwater flow is determined from the differential equation described in section 7, with τ_1 = 1 s and τ_2 = 1 s. The continued increasing of the feedwater flow is a result of the water level control term, which attempts to return the level to its original value. In fig. 11.d is finally shown the slight increase in feedwater temperature caused by the increasing pressure at the feedwater heater extraction points.

Fig. 11.e shows some characteristic quantities of the turbine and feedwater circuit. The first two curves show the pressure at inlet to the high-pressure turbine respectively low-pressure turbine. The curve of the high-pressure turbine almost follows the steam flow curve shown earlier in fig. 11.a, whereas the pressure at inlet to the low-pressure turbine reflects no overshoot because of the holdup time in the combined moisture separator-reheater. In the same way, the extraction flow to the heater nearest the reactor shows an overshoot, whereas the heater nearest the condenser, shown at the bottom of fig. 11.e, reflects a more smooth increase in the extraction flow.

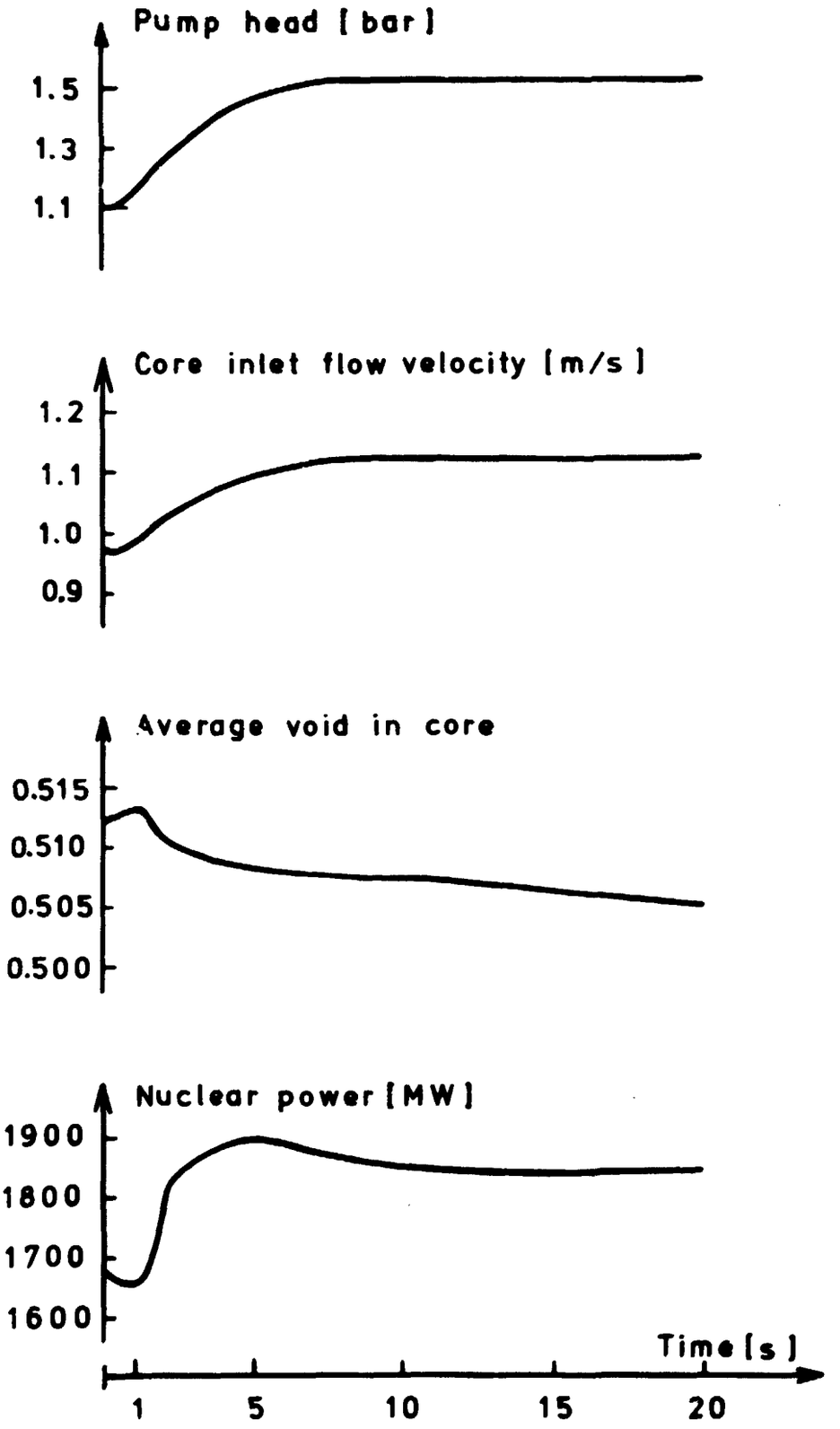

Fig. 11.b. Responses to a power demand from 560 MWe to 616 MWe within 1 s.

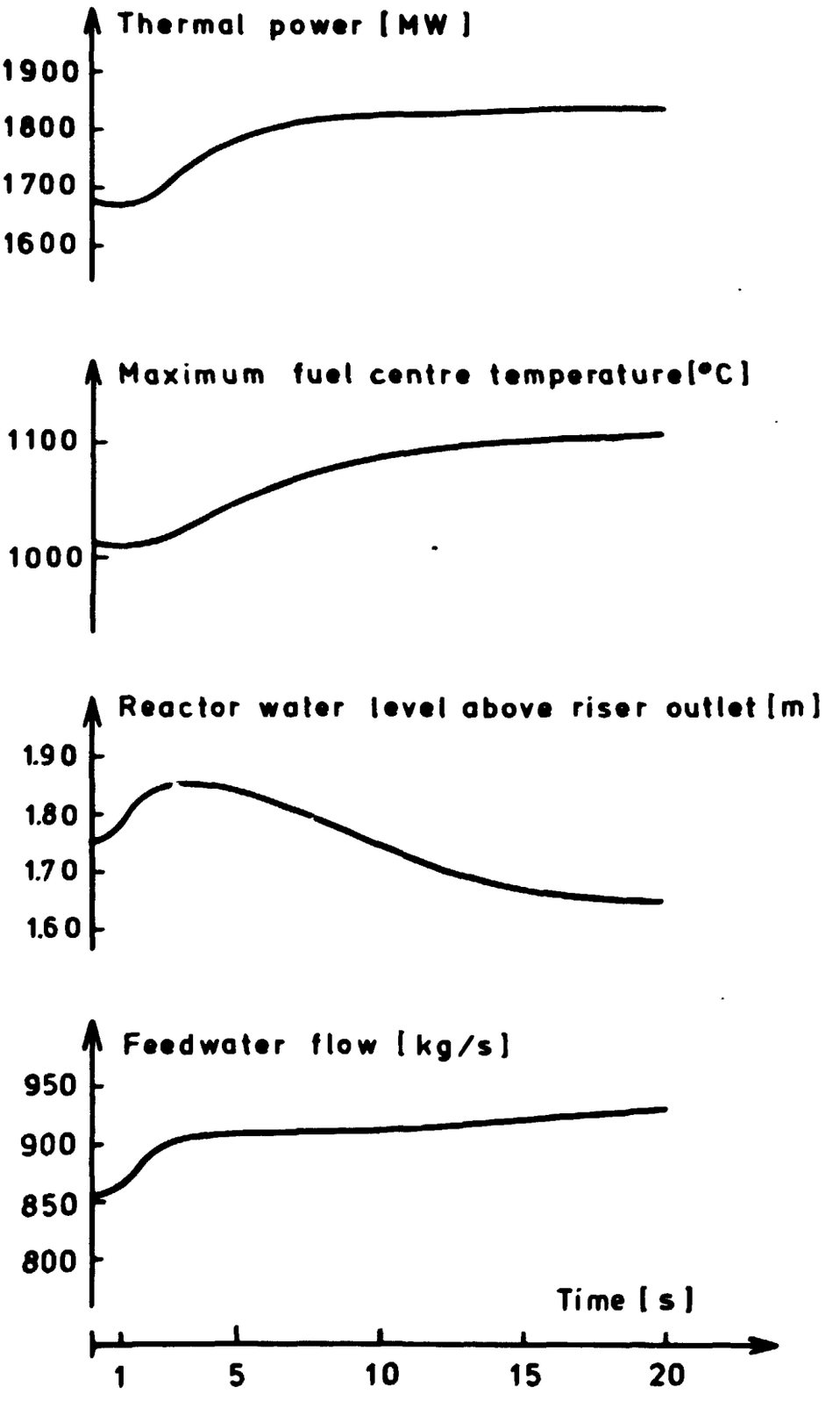

Fig. 11.c. Responses to a power demand from 560 MWe to 616 MWe within 1 s.

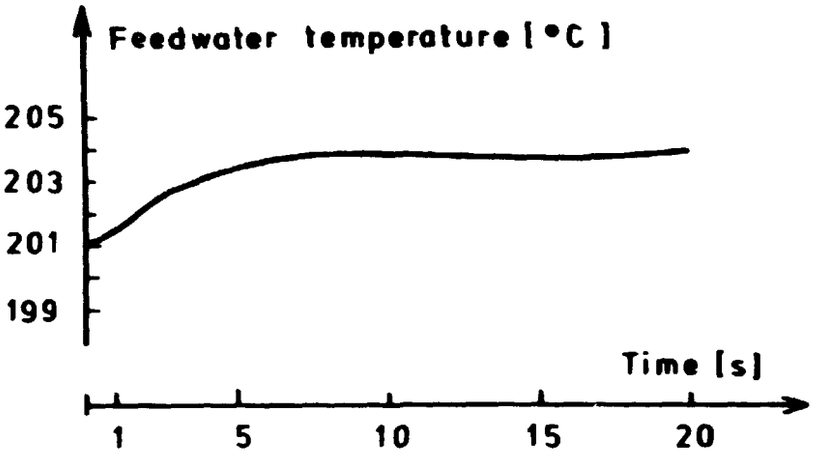

Fig. 11.d. Response of the feedwater temperature to a power demand from 560 MWe to 616 MWe within 1 s.

The regulation valve on the primary line to the reheater for keeping the reheater temperature constant shows almost no change in its position during the transient, and the same is the case for all the water level regulation valves in the feedwater heaters and drainage tanks.

Most of the results than can be obtained with the model have now been presented, in particular the effect of the different control systems has been demonstrated. Several other transients have been calculated, where the bypass control system has also been activated, but due to lact of time it is impossible to present them all. However, the considered transient should represent the applicability of the "BWRPLANT" model of a power plant based on a boiling water reactor.

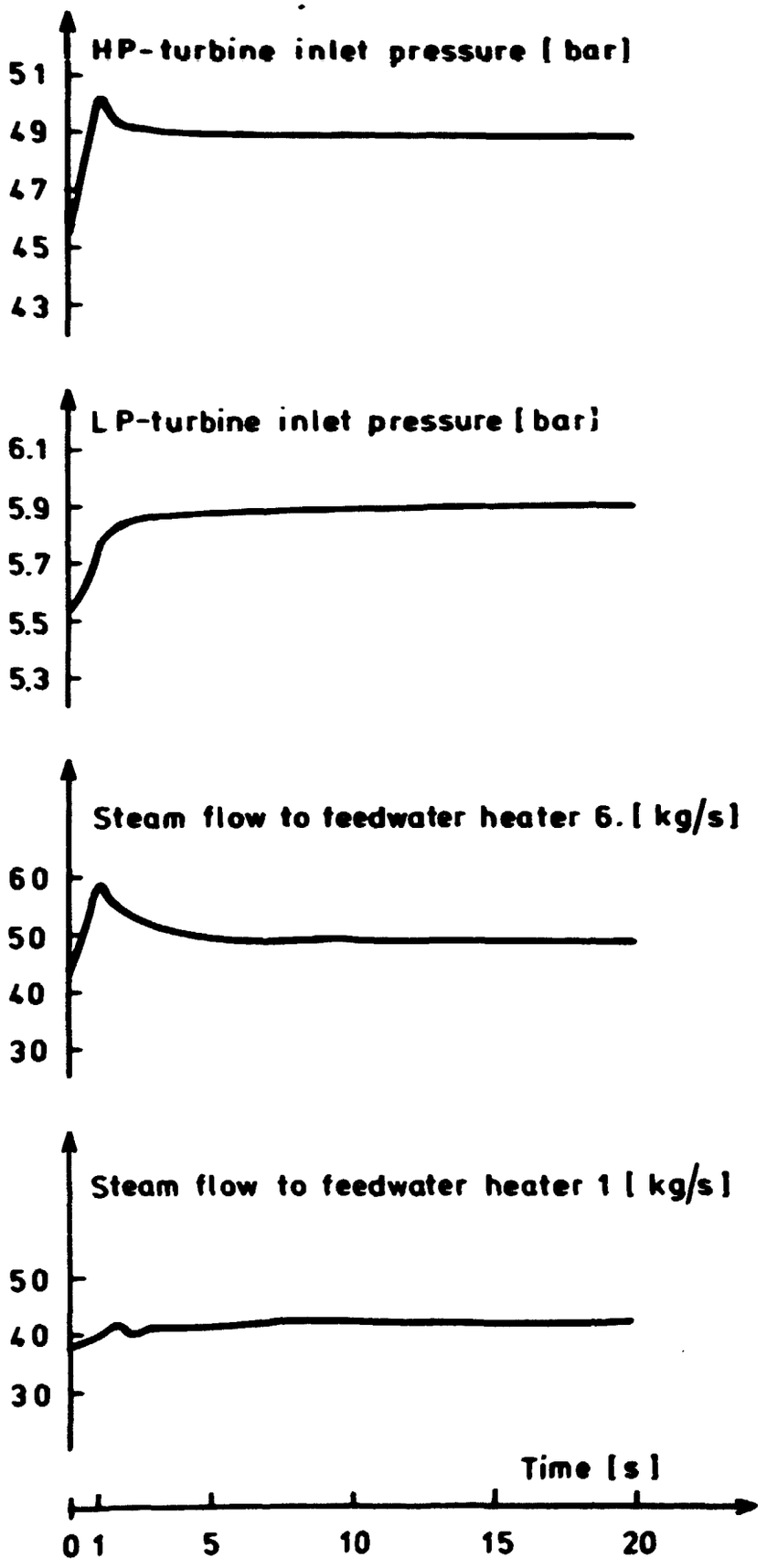

Fig. 11.e. Responses to a power demand from 560 MWe to 616 MWe within 1 s.

12. DISCUSSION AND CONCLUSION

The content of "BWRPLANT", a dynamic model of a nuclear power plant based on a boiling water reactor, has now been described and some results obtained with the model have been presented. The most important objection to the development of the plant model is the lack of verification against measurements on operating nuclear power plants. Numerous safety analysis reports were examined for experimental data on different transients and some data were found. But every attempt to verify the model against these experiments failed owing to insufficient information on the technical data of the specific nuclear power plants consituting the basis of the experiments. However, the reactor part of the model was tested indirectly against experiments through the comparison with the 3-dimensional model "ANDYCAP", because this model was earlier verified against experiments using the Swedish reactor Oskarshamn I.

The good agreement from this comparison is, in fact, surprising considering the difference in treatment of the reactors in the two models; but, as earlier mentioned, this could be a result of the fact that the chosen steam load perturbation causes no local effects in the reactor.

With respect to the transient treated in section 11, the results from here were compared to a similar transient for a 600 MWe BWR plant shown in ref. 9. The results seem to agree fairly well.

The main conclusion that can be drawn from the development of the dynamic model is its applicability for studying different transient incidents and control systems that are characteristic of a BWR nuclear power plant. This capability was demonstrated during the description of the model and can be further extended by including a model of the outside grid coupled to the plant. Both transients occurring during normal operation and transients caused, for example, by turbine trip, loss of condenser vacuum, malfunction of some control systems etc., the so-called "abnormal" transient incidents, can be studied. The main drawback when using the model is still, as described in part I, the demand for very detailed information on the technical data of the plant under consideration.

Finally, it should be mentioned that a more detailed treatment of the neutron kinetics part of the reactor model would be useful so as to avoid the calculation of the reactivity coefficients, thus to be independent of the "ANDYCAP" calculations, and to be able to include control rod movements.

13. ACKNOWLEDGEMENT

The author gratefully acknowledges the assistance of P. la Cour Christensen and M. Lind in the analysis of the regulation systems. Thanks are also due to P. Skjerk Christensen for valuable discussions and especially for his participation in the comparison using the 3-dimensional model.

APPENDIX A

The Matrix Exponential Method

The matrix exponential method is a procedure by which almost exact solutions are obtained for a system of first-order differential equations with constant coefficients, (ref. 10).

The differential equations are written as

$$\frac{dx_1}{dt} = a_{11}x_1 + a_{12}x_2 + \ldots\ldots\ldots\ldots a_{1n}x_n + z_1$$

$$\frac{dx_2}{dt} = a_{21}x_1 + a_{22}x_2 + \ldots\ldots\ldots\ldots a_{2n}x_n + z_2$$

$$\ldots\ldots\ldots\ldots\ldots\ldots\ldots\ldots\ldots\ldots\ldots\ldots\ldots\ldots\ldots\ldots$$

$$\ldots\ldots\ldots\ldots\ldots\ldots\ldots\ldots\ldots\ldots\ldots\ldots\ldots\ldots\ldots\ldots$$

$$\frac{dx_n}{dt} = a_{n1}x_1 + a_{n2}x_2 + \ldots\ldots\ldots\ldots a_{nn}x_n + z_n$$

or in matrix form

$$\frac{dX}{dt} = AX + Z ,$$

where Z represents the inhomogeneous term of the equation or the forcing function.

The homogeneous equation

$$\frac{dX}{dt} = AX$$

has the solution,

$$X_t = e^{At}X_o$$

which can be proved by expanding X_t in a Taylor series

$$X_t = X_o + t\left(\frac{dX}{dt}\right)_{t=o} + \frac{t^2}{2}\left(\frac{d^2X}{dt^2}\right) + \ldots\ldots \frac{t^k}{k!}\left(\frac{d^kX}{dt^k}\right)_{t=o} + \ldots\ldots$$

From

$$\frac{dX}{dt} = AX$$

we can derive

$$\frac{d^2X}{dt^2} = A^2X$$

and

$$\frac{d^kX}{dt^k} = A^kX .$$

Substitution in the Taylor series gives

$$X_t = X_o + AtX_o + (\frac{A^2t^2}{2})X_o + \ldots\ldots\ldots (\frac{A^kt^k}{k!})X_o + \ldots\ldots$$

or

$$X_t = \left[I + At + (\frac{A^2t^2}{2}) + \ldots\ldots\ldots (\frac{A^kt^k}{k!}) + \ldots\ldots \right] X_o ,$$

where I is the identity matrix. The solution thus becomes

$$X_t = e^{At}X_o$$

and the incremental solution

$$X_{t+\Delta t} = e^{A\Delta t}X_t .$$

If the inhomogeneous term Z_t can be considered as constant over the time interval t to $t + \Delta t$, a particular solution to the inhomogeneous equation can be written as

$$X_p = (e^{A\Delta t} - I)A^{-1}Z_t ,$$

which can be verified by substitution. Thus the final solution becomes

$$X_{t+\Delta t} = e^{A\Delta t}X_t + (e^{A\Delta t} - I)A^{-1}Z_t .$$

The calculation of the inverse matrix A^{-1} is not necessary since

$$(e^{A\Delta t} - I)A^{-1} = \left[I + A\Delta t + \frac{(A\Delta t)^2}{2} + \ldots\ldots \frac{(A\Delta t)^k}{k!} + \ldots\ldots - I\right]A^{-1}$$

$$= I\Delta t + \frac{A\Delta t^2}{2} + \frac{A^2\Delta t^3}{3!} + \ldots\ldots \frac{A^{k-1}\Delta t^k}{k!} + \ldots\ldots$$

$$= \Delta t \sum_{k=1}^{\infty} \frac{(A\Delta t)^{k-1}}{k!}$$

The matrix $e^{A\Delta t}$ can be written as

$$e^{A\Delta t} = \sum_{k=o}^{\infty} \frac{(A\Delta t)^k}{k!} .$$

Putting $e^{A\Delta t} = C$ and $(e^{A\Delta t} - I)A^{-1} = HP$, the final solution can be expressed by

$$X_{\Delta t} = CX_o + HPZ_o$$

$$X_{2\Delta t} = CX_{\Delta t} + HPZ_{\Delta t}$$

.....

.....

$$X_{n\Delta t} = CX_{(n-1)\Delta t} + HPZ_{(n-1)\Delta t} .$$

The advantage of this method is that, with the time increament Δt constant during the integration, the matrices C and HP need to be evaluated once only and thus the method is very rapid. In order to ensure convergence of the series expansion of $e^{A\Delta t}$, the following condition must be fulfilled

$$\max \left| A_{i,j}\Delta t \right| < 1.0 ,$$

and thus a limit is fixed to the size of the time step t. The numerical accuracy of the method can be increased almost arbitrarily by including an increasing number of terms in the Taylor series of $e^{A\Delta t}$; the accuracy of the computer used determines the limit.

Finally, it should be mentioned that, in the plant model developed, the matrix A varies very slowly, and the matrices C and HP are therefore recalculated whenever any of the elements in A have altered by some present fraction subsequent to the last evaluation.

APPENDIX B

Determination of the Numerical Values of the Control Parameters by Means of Classical Frequency Analysis

An example of the determination of the parameters of the recirculation system will now be given. The values calculated are those used in the transient described in section 11. The method used is a determination of transfer functions and a frequency analysis of these together with Nyquist's stability criterion (ref. 11).

In order to determine the transfer function for the response of the nuclear power to a change in the pump valve position, a step was applied in the last quantity.

During this responce of the nuclear power the pressure regulator was controlling the reactor pressure.

The response of the nuclear power to this step in pump valve position is shown in fig. B.1. In order to obtain a Laplace representation of this response curve, it was simulated at the Risø analogue computer. A computer program based on state-space technique (ref. 12) was then used to calculate the coeffi:ients of the transfer function with the following result

$$H(s) = \frac{202s + 0.954}{s^3 + 1.35s^2 + 6.11s + 2.34} .$$

After the transfer function from the pump valve position to the nuclear power had been determined, an examination was made of three different types of regulator normally used

a) P-regulator

b) PI-regulator

c) PID-regulator.

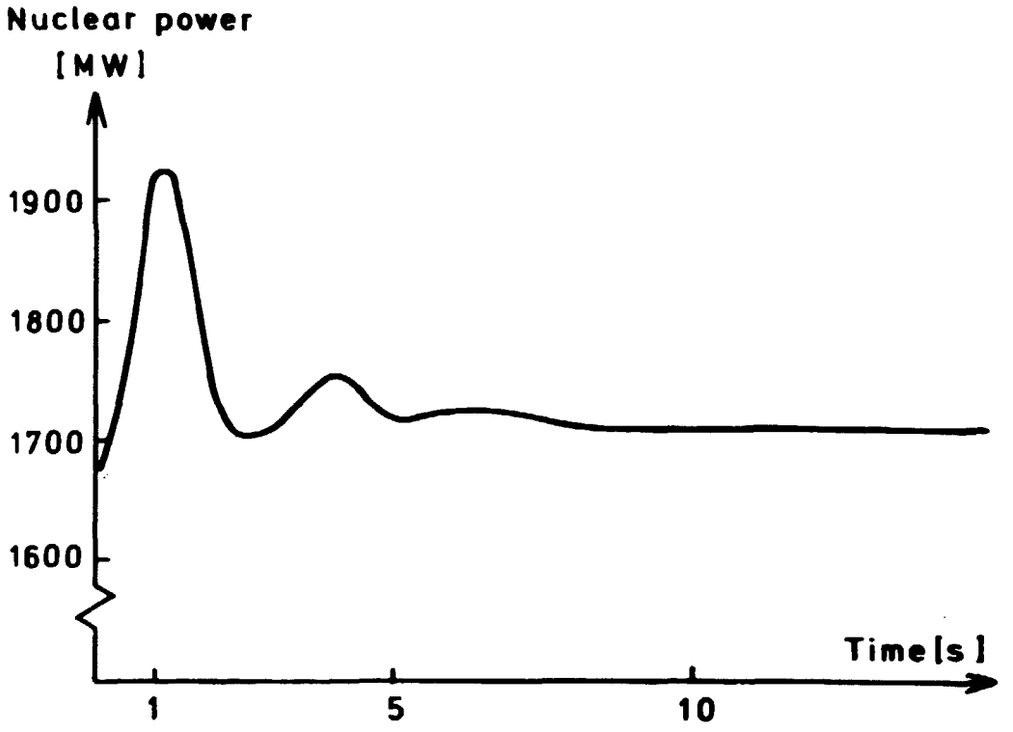

Fig. B.1. The response of the nuclear power to a jump in the pump valve position.

a. A Proportional Regulator

The pump valve is adjusted by the proportional regulator using the difference between the required nuclear power N_{set} and the actual power N. The control diagram is shown in fig. B.2.

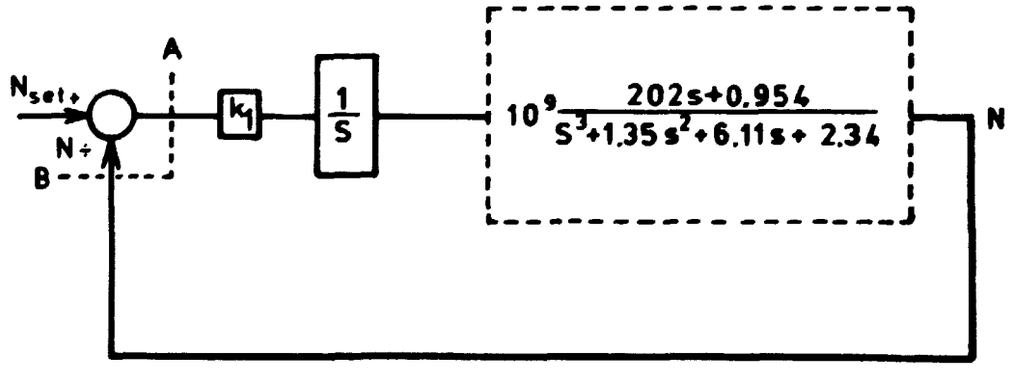

Fig. B.2. Diagram of the flow control system using a P-regulator.

The transfer function H(s) defined by

$$H(s) = \frac{B(s)}{A(s)}$$

with the feedback line open at B, also called the open loop transfer function, is now determined and a frequency analysis is carried out. During this analysis the value of k_1 is set equal to $2.0 \cdot 10^{-10}$; a more exact value will be determined later. The calculation is carried out by the state-space variable program mentioned above, and the transfer function becomes

$$H(s) = \frac{3.86s + 0.182}{s^4 + 1.35s^3 + 6.11s^2 + 2.34s} .$$

In fig. B.3 is shown a Nyquist plot, i.e. a frequency response of the open loop transfer function in an H-plane with the axes Re(H(iω) and Im(H(iω)) and the frequency ω going from $-\infty$ to $+\infty$. Nyquist's stability criterion now states that if H(iω) does not encircle the point (-1.0), the system is stable. It is thus seen from fig. B.3 that the proportional regulator system is stable with the chosen value of k_1, and even if k_1 is multiplied by 1.5 the stability is ensured.

Later in this appendix a transient will be calculated with the described P-regulator and k_1 equal to $3.0 \cdot 10^{-10}$.

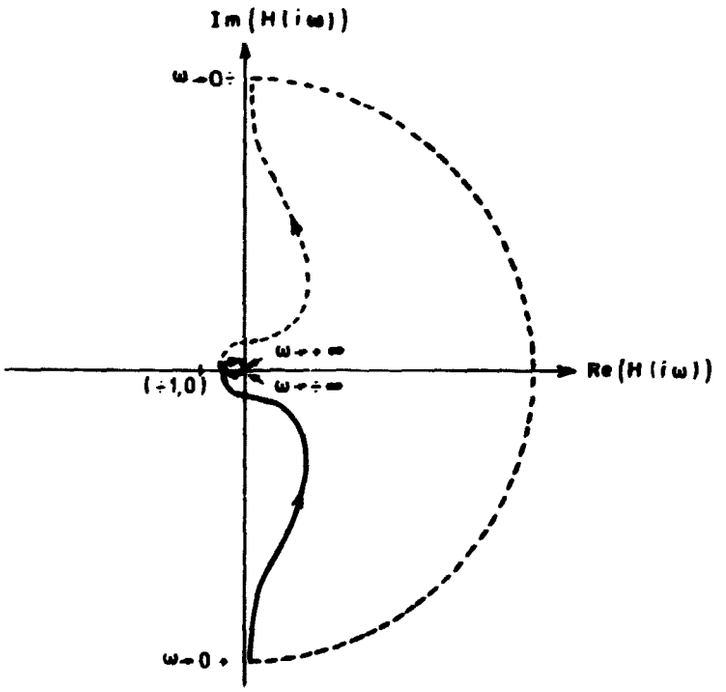

Fig. B.3. Nyquist plot of the open loop transfer function using a P-regulator.

b. A Proportional and Integrating Regulator

If a PI-regulator is chosen for adjusting the pump valve, the control system becomes

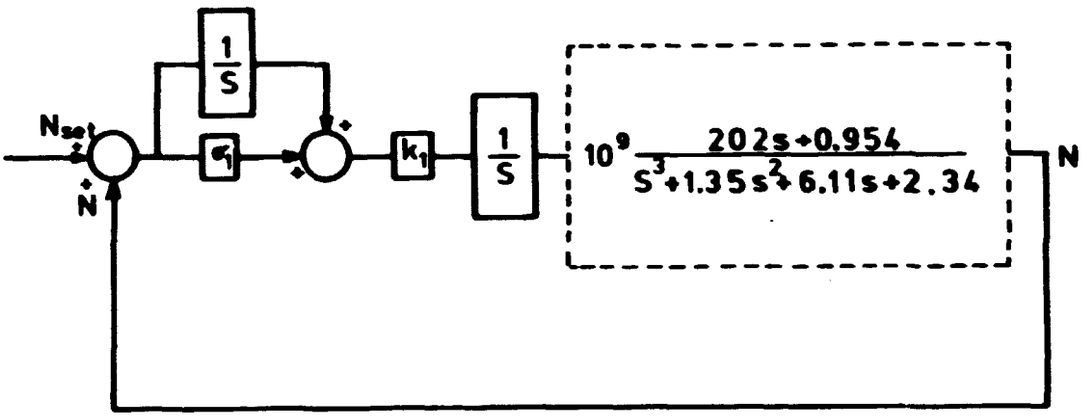

Fig. B.4. Diagram of the flow control system using a PI-regulator.

The open loop transfer function is calculated similarly to that described for the P-regulator. With $k_1 = 3.0 \cdot 10^{-10}$ and $\sigma_1 = 0.05$, the transfer function becomes

$$H(s) = \frac{3.86s^2 + 4.05s + 0.18}{s^5 + 1.35s^4 + 6.11s^3 + 2.34s^2} .$$

The Nyquist plot of the transfer function is shown in fig. B.5. The system is seen to be stable with the chosen values of the parameters k_1 and σ_1 according to Nyquist's stability criterion, but the stability margin is less than for the P-regulator. By reducing the value of k_1, the margin can be increased however.

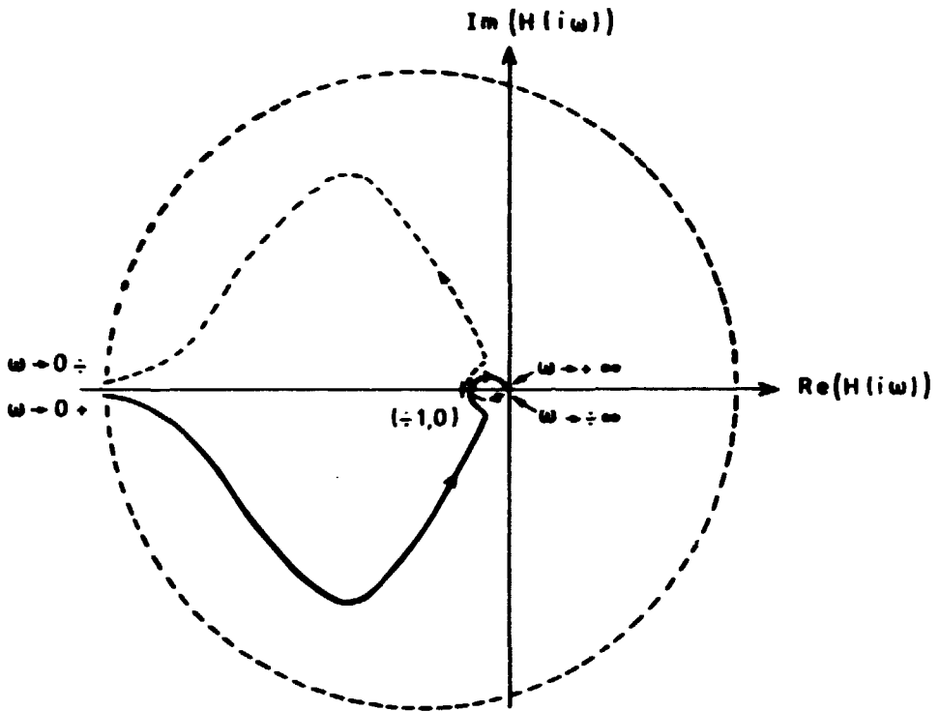

Fig. B.5. Nyquist plot of the open loop transfer function using a PI-regulator.

c. A Proportional, Integrating and Differentiating Regulator

Finally, the PID-regulator shown in fig. B.6 is treated. The open loop transfer function is calculated to

$$H(s) = \frac{3.86s^2 + 4.05s + 0.182}{s^5 + 1.35s^4 + 9.47s^3 + 2.51s^2 + 6.5 \cdot 10^{-3}s},$$

and the Nyquist plot is shown in fig. B.7. The values of the parameters σ_1, k_1, and τ_1 were set to 1.0, $3.0 \cdot 10^{-10}$ and 0.5, and again it appears that the system is stable, even with a greater stability margin than was the case for the PI-regulator.

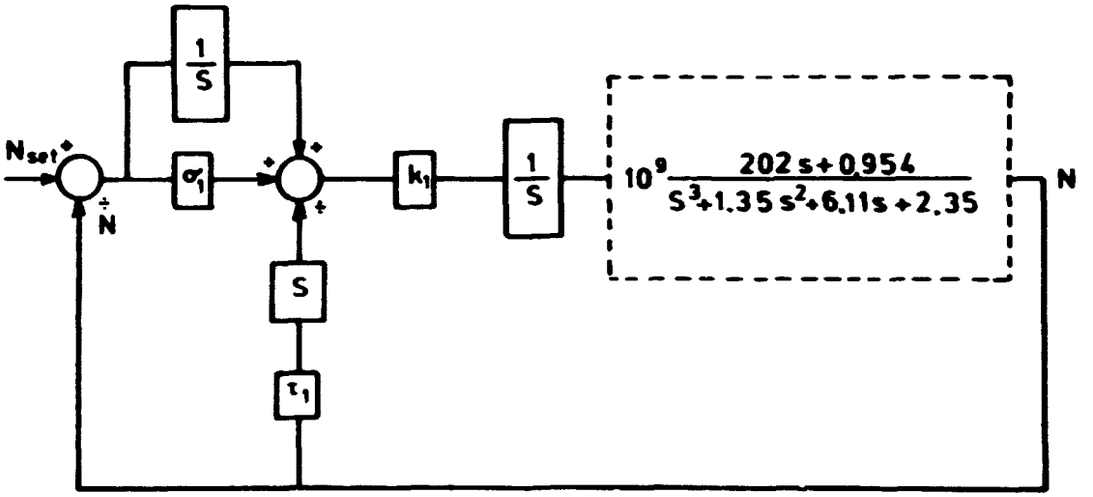

Fig. B. 6. Diagram of the flow control system using a PID-regulator.

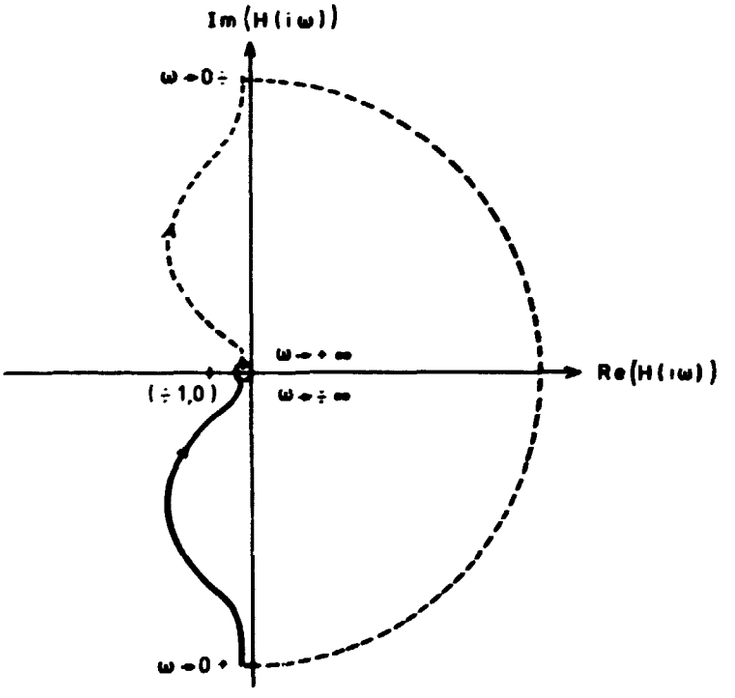

Fig. B. 7. Nyquist plot of the open loop transfer function using a PID-regulator.

In fig. B.8 is shown a transient calculated with the three different regulators; the dashed curve represents the required power. All the curves are damped, but the PID-regulator seems to approximate the required power best without too many oscillations. Other transients made also seem to indicate that the PID-regulator is preferable for controlling the nuclear power according to the required power, through a change of the recirculation pump valve position. This result was the reason for the choice of the PID-regulator in the transient described in section 11. However, through a more detailed investigation of the influence of the parameters σ_1, k_1 and τ_1, a still better regulator might be obtained.

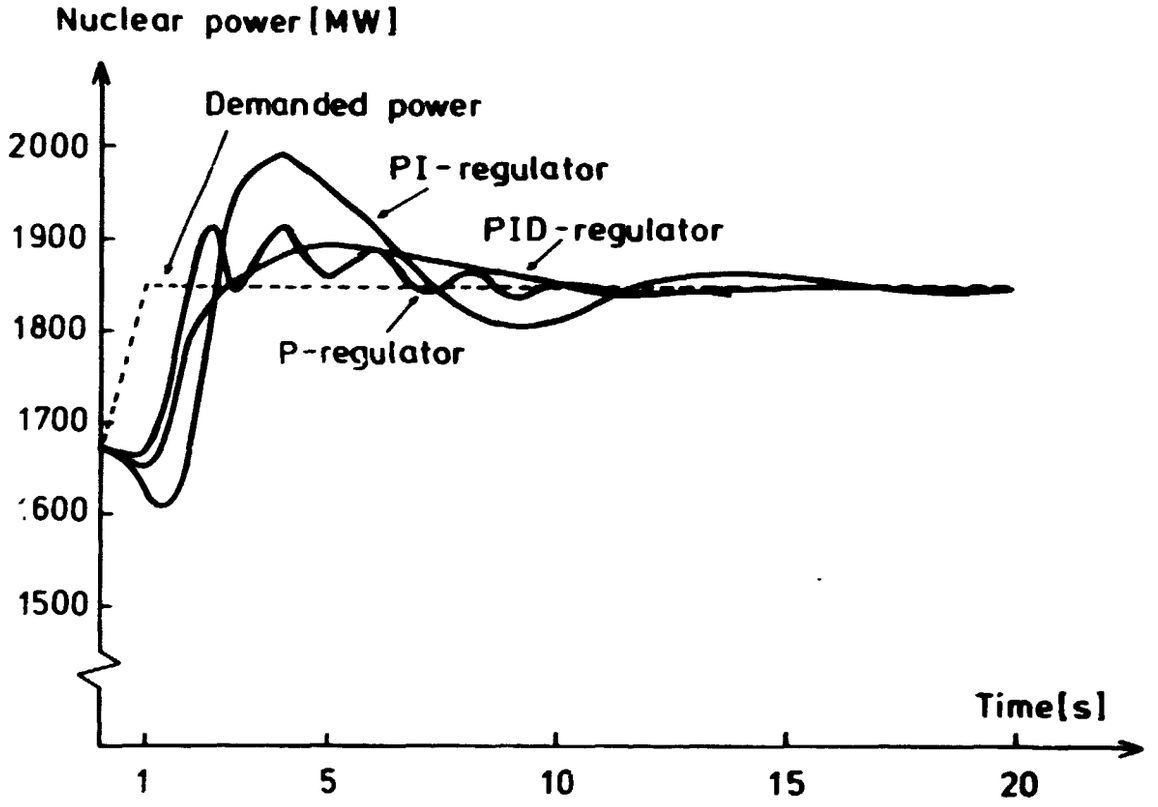

Fig. B.8. The response of the nuclear power to the power increase, mentioned in section 11, from 560 MWe to 616 MWe within 1 s using three different types of regulators.

By using the same technique as outlined in this appendix, the parameters of the pressure control system were determined and a PD-regulator was found to be sufficient.

Since the two main regulation systems, the pressure control systems and the flow control system, interact with each other, a new analysis of the recirculation flow control system should be made when the pressure control parameters are calculated and vice versa, but this is beyond the scope of the present report.

REFERENCES

1) P. Bakstad, and K. O. Solberg, A Model for the Dynamics of Nuclear Reactors With Boiling Coolant With a New Approach to the Vapour Generating Process. KR-121 (1967) 79 pp.

2) W. Traupel, Thermische Turbomaschinen Bd. I 2. Aufl. (Springer-Verlag, Berlin, 1966) 522 pp.

3) W. Traupel, Thermische Turbomaschinen Bd. II 2. Aufl. (Springer-Verlag, Berlin, 1968) 507 pp.

4) J.G. Delene, A Digital Computer Code for Simulating the Dynamics of Demonstration Size Dual-Purpose Desalting Plants Using a Pressurized Water Reactor as a Heat Source. ORNL-TM-4104 (1973) 128 pp.

5) D. M. Young, and R. T. Gregory, A Survey of Numerical Mathematics Vol. I (Addison-Wesley-Publishing Company, Reading, Mass., 1972) 492 pp.

6) J. Grimson, Mechanics and Thermodynamics of Fluids (McGraw-Hill Publishing Company, Maidenhead, U. C.) 343 pp.

7) BWR/6 Standard Safety Analysis Report, Docket STN-50-447. Loose leaf.

8) L. Lapidus, and J. H. Seinfeld, Numerical Solution of Ordinary Differential Equations (Academic Press, New York, 1971) 299 pp.

9) A. Sauer, Siedewasserreaktoren für Kernkraftwerke (AEG-Telefunken, Berlin, 1969) 164 pp.

10) S.J. Ball, and R. K. Adams,"MATEXP" A General Purpose Digital Computer Program for Solving Ordinary Differential Equations by the Matrix Exponential Method. ORNL-TM-1933 (1967) 60 pp.

11) P. M. DeRusso, R. J. Roy, and C. M. Close, State Variables for Engineers (John Wiley and Sons Inc., New York, 1965) 608 pp.

12) Z. Akcasu, G. S. Lellouche, and L. M. Shotkin, Mathematical Methods in Nuclear Reactor Dynamics (Academic Press, New York, 1971) 460 pp.

ISBN 87-550-0406-7